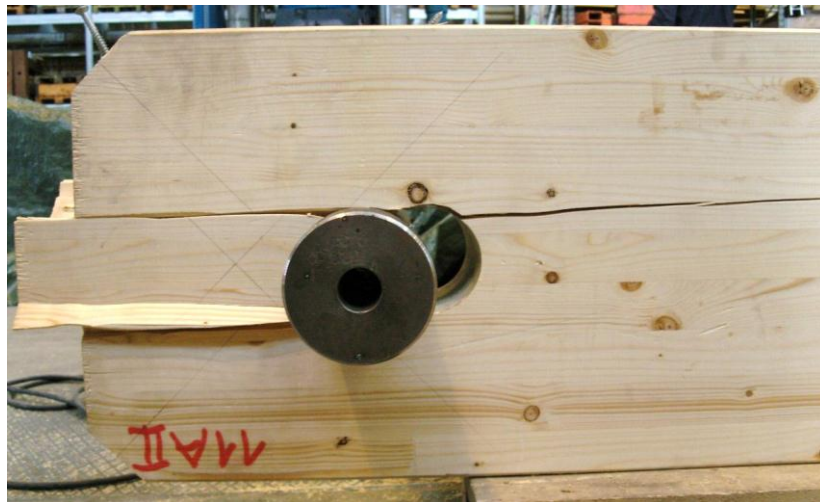


# Modelling of Strengthened Connections for Large Span Truss Structures



**Peter Kobel**

---

Avdelningen för Konstruktionsteknik  
Lunds Tekniska Högskola  
Lunds Universitet, 2011

Rapport TVBK - 5198

Avdelningen för Konstruktionsteknik  
Lunds Tekniska Högskola  
Box 118  
221 00 LUND

Department of Structural Engineering  
Lund Institute of Technology  
Box 118  
S-221 00 LUND  
Sweden

## **Modelling of strengthened connections for large span truss structures**

Peter Kobel

2011

Rapport TVBK-5198  
ISSN 0349-4969  
ISRN: LUTVDG/TVBK-11/5198+91p

Examensarbete  
Handledare: Roberto Crocetti  
Juni 2011

## **Preface**

This report was written as a master's thesis at the Institute of Structural Engineering at ETH Zürich, Switzerland. The work was performed in the course of a student exchange from March till July 2011 at the Division of Structural Engineering at Lund University/LTH, Sweden. It was performed in cooperation with SP-Trätekt in Borås, Sweden.

I would like to thank my supervisor Prof. Dr. Roberto Crocetti from Lund University for giving me the opportunity to perform the thesis in Sweden as well as for his supervision of the work. Further thanks go to Prof. Dr. Andrea Frangi from ETH Zürich for his support and to Mats Axelson from SP-Trätekt for his supervision of the laboratory tests and his active support in testing.

Lund, July 2011

Peter Kobel



## **Abstract**

Because of its large ratio between strength and weight timber is a material very suitable for large span structures. For large spans of more than about 30 m, usually truss structures are adopted. The problem of large span timber truss structures are the expansive and complex nodes that have to be adopted, normally single or multiple slotted-in steel plates in combination with a number of dowels.

In order to find a more efficient and economical solution for timber nodes, a novel truss node has been developed at SP-Träteknik in Borås. The node consists of a single large-diameter dowel which connects the diagonals with the chords. Additionally, self-tapping reinforcing screws are applied to prevent premature splitting failure and also to increase the strength and the stiffness of the node.

In the course of this thesis a full-scale test series was carried out to investigate the behaviour of the node. 15 glulam specimens with reinforced single large-diameter dowel connections were tested in load controlled tensile tests. Besides various configurations of self-tapping screws also lateral prestressing was used as a reinforcement measure.

It was found that the bearing capacity of the connection can be significantly increased by applying self-tapping screws. Reinforcing screws effectively impede splitting of the timber if placed near the loaded end of the connection, where major lateral deformations occur. However, reinforcing screws cannot prevent the formation of a shear plug, which was observed to be the ultimate failure mode.

Lateral prestressing of the connection also proved to be an effective reinforcement measure, as splitting can be prevented completely. By applying large lateral prestresses the failure mode changes to a combined shear and tensile failure which results in a higher bearing capacity.



# Contents

Preface.....	i
Abstract .....	iii
1 Introduction and Aims of the Thesis .....	1
2 Theoretical Background .....	5
2.1 State of the Art.....	5
2.1.1 Johansen’s Yield Theory .....	5
2.1.2 Further Studies .....	7
2.2 Preliminary Small-Scale Test Series .....	9
3 Laboratory Tests.....	13
3.1 Introduction .....	13
3.2 Specimens and Reinforcements .....	15
3.2.1 General .....	15
3.2.2 Specimen Group “Basic” .....	16
3.2.3 Specimen Group “A2+B2” .....	17
3.2.4 Specimen Group “02+A2” .....	18
3.2.5 Specimen Group “Inclined” .....	20
3.2.6 Specimen Group “Dywidag” .....	21
3.3 Test Setup .....	24
3.3.1 Setup and Loading Procedure .....	24
3.3.2 Measurements.....	27
4 Results .....	29
4.1 Annotations.....	29
4.2 Results Group “Basic” .....	31



4.3	Results Group “A2+B2” .....	34
4.4	Results Group “O2+A2” .....	37
4.5	Results Group “Inclined” .....	40
4.6	Results Group “Dywidag” .....	43
4.7	Summary of Test Results .....	47
4.7.1	Bearing Capacity .....	48
4.7.2	Failure Mode.....	48
4.7.3	Stiffness and Dowel Slip .....	49
4.7.4	Splitting and lateral stiffness .....	50
5	Discussion.....	53
5.1	Bearing Capacity and Lateral Deformations .....	53
5.1.1	Connections Reinforced with Screws .....	53
5.1.2	Prestressed Connections .....	55
5.2	Stiffness.....	55
5.3	Comparison with Preliminary Test Series .....	56
5.4	Failure Process and Failure Mode.....	57
5.4.1	Simplified Model for Resistance Against Shear Failure.....	57
5.4.2	Comparison Between Groups “Basic” and “A2+B2” .....	59
5.4.3	Failure Modes in Prestressed Connections .....	64
6	Conclusions and Future Work .....	69
7	References.....	71
8	Appendix .....	1
	A1 Bearing Capacities .....	1
	A2 Stiffness Values (Load – Dowel Slip).....	1
	A3 Splitting.....	1

A4 Lateral Stiffness .....	1
A5 Densities and Moisture Contents .....	1
A6 Failure Modes .....	1



## 1 Introduction and Aims of the Thesis

Timber is an outstanding material when it comes to large span structures. In terms of statics, the main quality of timber is its large ratio between strength and weight. This ratio is extremely favourable for timber compared to other building materials and it makes timber therefore suitable for large spans.

For large spans of more than about 30 m, usually truss structures are adopted. Timber trusses with a span up to 100 m have already been erected, e.g. for the Olympic Games in Lillehammer. However, the problem of large span timber truss structures are usually the expansive and complex nodes that have to be adopted. This is mainly due to the brittle behaviour of timber and its low lateral tensile strength which leads to an enhanced risk of splitting phenomena. Usually, single or multiple slotted-in steel plates are used in combination with a number of dowels to form the truss nodes. These types of nodes imply a considerable amount of steel material in the connection as well as a rather complex manufacturing process. Furthermore, the dimensions of the connection can lead to overdimensioning of the joined timber members. As a consequence, truss structures in timber are often not able to compete economically with solutions in other materials (e.g. steel) for large spans.

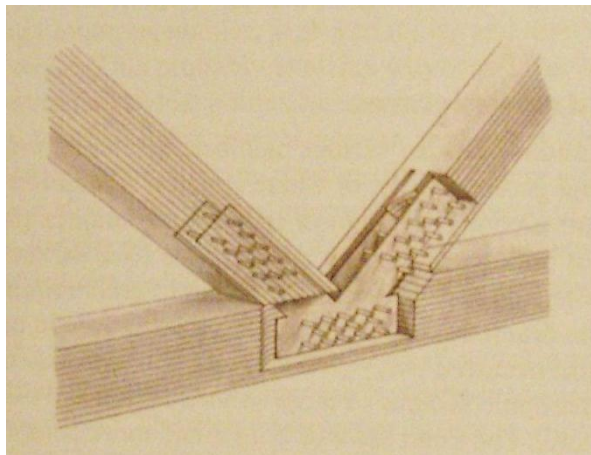


*Figure 1 Typical timber truss node with slotted-in steel plates and dowels. (Dahl, 2009)*

In order to find a more efficient and economical solution for timber nodes, a novel truss node has been developed at SP-Trätekt in Borås. The node consists of a single large-diameter dowel which connects the diagonals with the chords. Additionally, self-tapping reinforcing screws are applied to prevent premature splitting failure and also to increase the strength and the stiffness of the node.

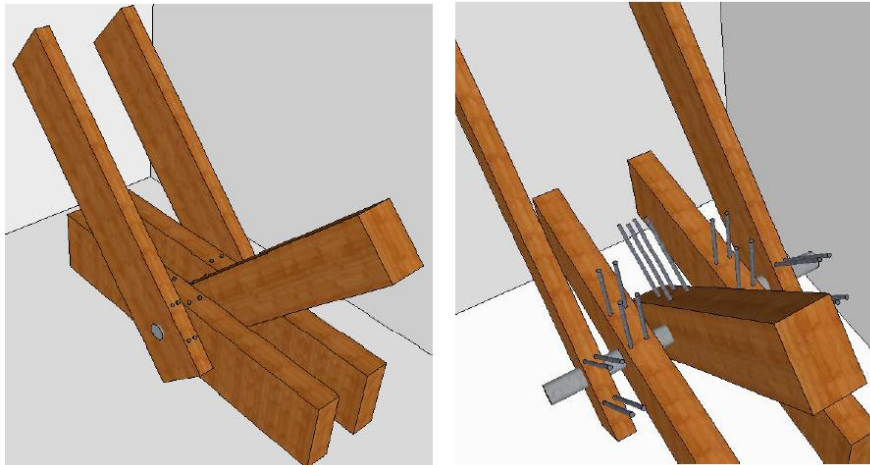


*Figure 2 Concept of the novel truss node developed at SP-Trätekt Borås.*

A practical problem of connections using large dowels is the end distance. The minimal end distance after Eurocode 5 (2004) is  $a_3 = 7d$ , i.e. the distance between the dowel axis and the loaded end has to be at least seven times the dowel diameter. For large dowel diameters this means that the end distance becomes very long, leading to additional material requirement. Furthermore, the long end distances can be impractical within the construction. The dowels used in the test series conducted for this thesis were 90 mm in diameter, meaning the required end distance after Eurocode would be  $a_3 = 7d = 63$  cm.

Because of these practical problems of large-dowel connections, the end distance in the newly developed node was reduced to half of the value suggested by Eurocode. Thus, in the test series conducted for this thesis, the end distance was set to  $a_3 = 3,5d$ . This measure reduces the practical problems mentioned above. However, the risk for splitting along the grain increases by not abiding by the end distance prescribed by Eurocode, which makes the use of lateral reinforcements necessary.

The aim of the thesis is to investigate the overall behaviour of the node. This includes bearing capacity, stiffness values as well as determining the occurring failure modes. Thereby, the process of premature splitting is of major interest as reduced end distances between the dowel and the loaded end are used. Ultimately, the aim is to evaluate suitable reinforcing measures for the connection. A major part of the work for this thesis was to conduct a full-scale test series at SP-Träteknik in Borås and to get information about the behaviour of the node by analysing the collected data.



## 2 Theoretical Background

### 2.1 State of the Art

#### 2.1.1 Johansen's Yield Theory

The most established theory for timber connections with dowel-type fasteners was published by K.W. Johansen (1949). Johansen's yield theory has since been adopted in building codes like Eurocode 5. It derives the load-carrying capacity of the connection from equilibrium conditions within the joint. Two different types of failure are considered. Failure occurs either if the embedding strength of the timber or the bending capacity of the fastener is reached. These two types of failure are combined to different failure modes of the connection, depending on the geometry, the material properties and other boundary conditions of the node.

In terms of geometry the failure mode depends on the number of shear planes, the thickness of the timber members and the dimensions of the fastener. An important factor is also the ratio  $\lambda = t/d$  between the thickness  $t$  of the timber member and the dowel diameter  $d$ .  $\lambda$  determines the slenderness of the fastener and has an influence on the distribution of the embedment stress.

The critical values linked to material properties are the embedding strength of the timber and the yield moment of the fastener. The embedding strength is dependent on the timber density and the fastener diameter, whereas the yield moment is determined by the yield stress of the fastener material as well as the fastener diameter. Johansen's yield theory is based on the assumption of rigid-plastic material properties (Figure 3). This is assumed for the timber material under embedding stress as well as for the dowel under bending action.



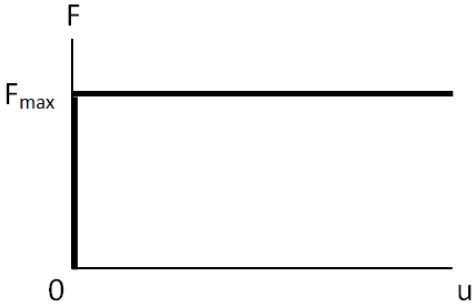


Figure 3 Idealised rigid-plastic behaviour.

Additional boundary conditions have to be taken into account for steel-to-timber connections. Depending on the thickness of the used steel plates the connection between the plate and the fastener is either considered to be a fixed support (thick steel plate) or a pinned support (thin steel plate). A fixed support means that additional plastic hinges in the fastener are formed at the plate surface.

Based on these assumptions, a number of possible failure modes can be derived for timber-to-timber connections as well as for steel-to-timber connections with one or multiple shear planes. By setting up equilibrium equations for forces and moments, the load-carrying capacity is derived for each failure mode. An example is shown in Figure 4 where the failure modes for single and double shear timber-to-timber joints are displayed.

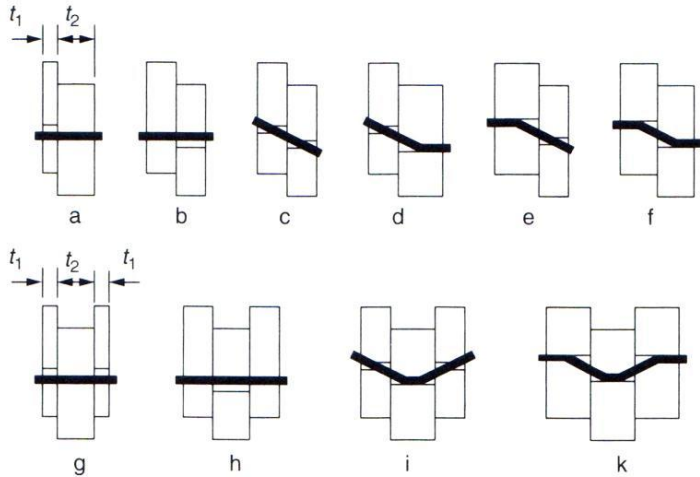


Figure 4 Failure modes for timber-to-timber joints after Johansen.

A fact which is particularly important for this thesis is that splitting along the grain and shear failure in the timber were not considered as possible failure modes by Johansen. In Eurocode this is taken into account by introducing a minimal end distance  $a_3 = 7d$  between the dowel axis and the loaded end. In this way, the failure modes of splitting and shear failure are excluded. However, if reduced end distances are used these additional failure modes have to be considered.

### 2.1.2 Further Studies

Jorissen (1998) has done some extensive studies on stress distribution in connections with dowel-type fasteners. To study the stresses perpendicular to the grain Jorissen divided the timber member in parts which were modelled as beams on elastic foundations (Figure 5). For the performed elastic calculations, the discontinuity due to the dowel hole and possible cracks were neglected. Additionally to the stresses from this model, Jorissen assumed peak stresses near the dowel, in order to take into account the influence of the fastener. Superposition of the stresses derived from the elastic beam model with the assumed peak stresses near the fastener led to the stress distribution shown in Figure 6. According to Jorissen, the peak tensile stresses perpendicular to the grain occur near the fastener and consequently splitting of the timber is predicted to be initiated at the fastener. The stress analysis by Jorissen was carried out for fasteners up to 20 mm in diameter.

Furthermore, Jorissen did some analysis on shear stresses within the connection, finding maximum shear stresses near the fastener and decreasing stresses towards the loaded end.

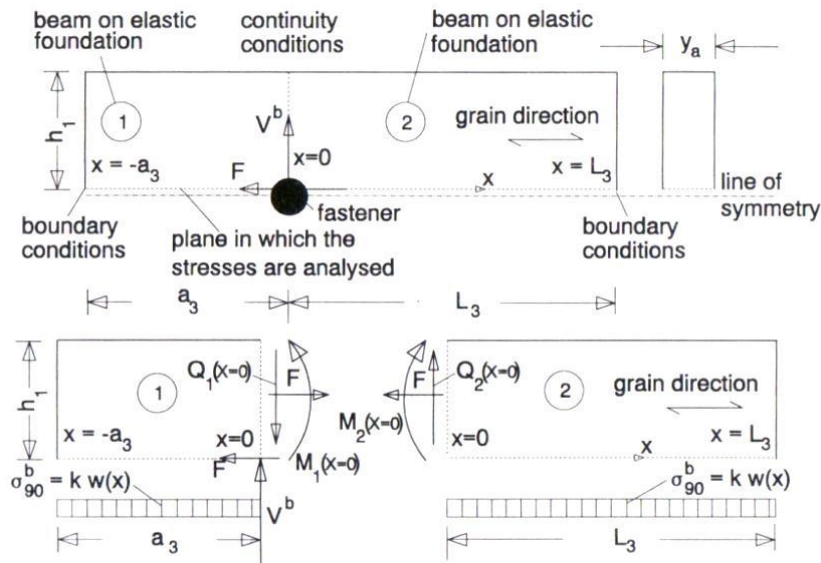


Figure 5 Model for the determination of stresses perpendicular to the grain. (Jorissen, 1998)

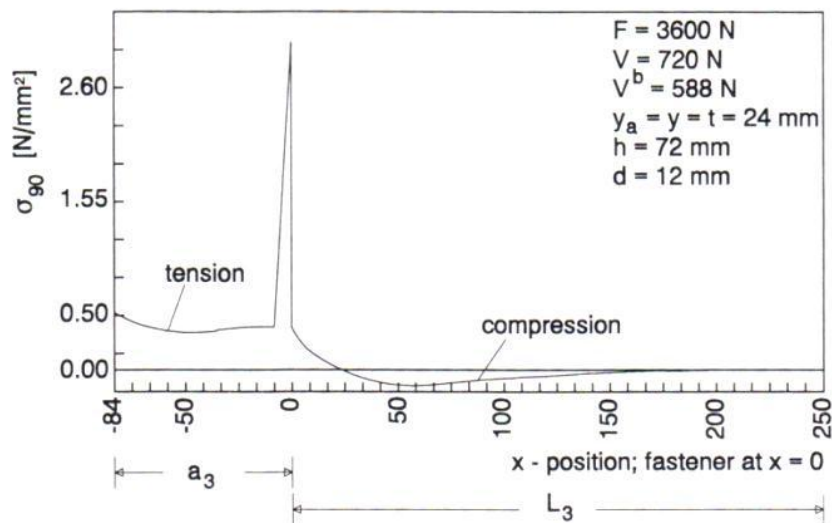


Figure 6 Stresses perpendicular to the grain including the approximated peak stresses.

Bejtka (2005) has studied connections with dowel-type fasteners reinforced with self-tapping screws. As seen in Figure 7 the connection was modelled as a beam on elastic foundation. Bejtka added reinforcing screws to the system and assumed a crack starting from the dowel. Bejtka's studies showed that self-tapping screws can be used to efficiently reinforce connections with dowel-type fasteners.

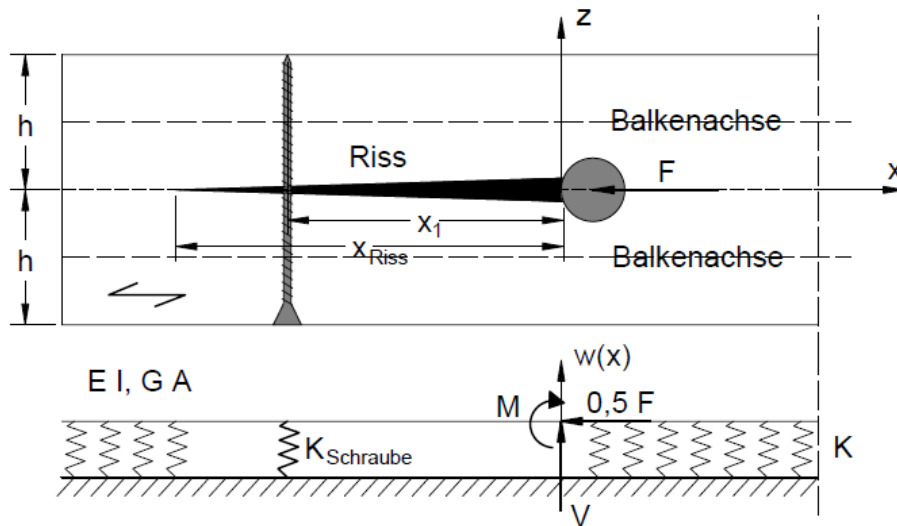


Figure 7 Model of a reinforced connection. (Bejtka, 2005)

Blass and Bejtka (2008) have further developed numerical methods to determine the bearing capacity and the stiffness of reinforced connections with dowel-type fasteners.

## 2.2 Preliminary Small-Scale Test Series

As a pre-study to the full-scale test series performed in the course of this thesis a preliminary small-scale test series was carried out by Crocetti, Axelson and Sartori (2010). 26 spruce specimens were tested in displacement controlled tensile test. The load direction was parallel to the grain. The cross section of the specimens was 45 mm × 140 mm and the steel dowel had a diameter of 32 mm. The end distance was set to 3,5 times the diameter of the dowel (Figure 8).

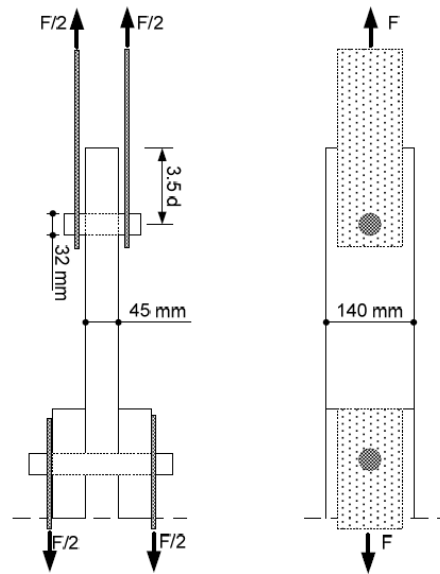


Figure 8 Test setup. (Crocetti, Axelson, & Sartori, 2010)

A reference group of five specimens was tested without any reinforcements. All other specimens were reinforced with self-tapping screws inserted perpendicularly to the dowel and also perpendicularly to the grain (Figure 9). Most of the screws had a diameter of 6,3 mm, although in some specimens also screws with diameters of 10 mm and 13 mm were used. To prevent splitting at the end grain during insertion of the reinforcing screws, smaller secondary screws ( $d = 4$  mm) were placed in advance. The reinforcing screws were placed in various combinations on three different levels between the dowel and the loaded end. In total, eight different configurations of reinforcement screws were tested.

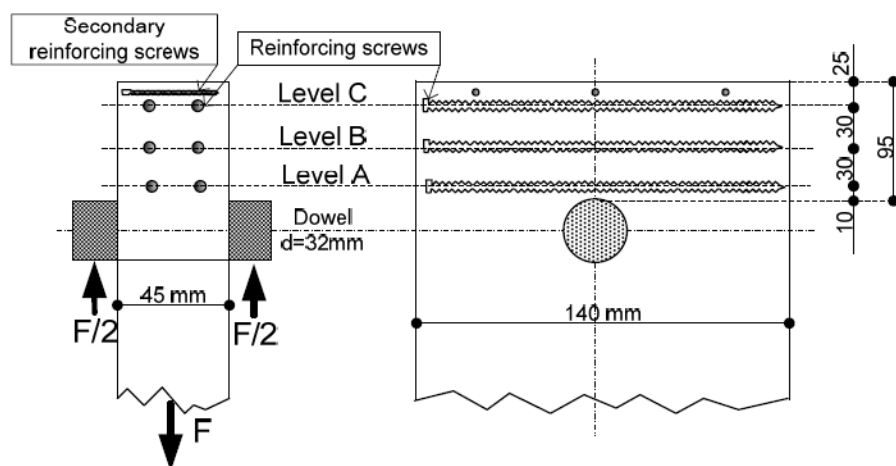


Figure 9 Placement of reinforcing screws in the specimen. (Crocetti, Axelson, & Sartori, 2010)

Specimen group	$N$	$P_{max}$ [kN] ( $\delta_{max}$ ) [mm]	CoV	$P_{ult}$ [kN]	$P_{\delta=5}$ [kN]	$k$ [N/mm]	$\rho$ [kg/m <sup>3</sup> ]
Non-reinforced	5	20.9 (1.0)	0.7	20.9	0.0	26164	459
A(1_d6.3)	3	41.2 (1.6)	0.03	43.5	25.3	39960	485
A(1_d13_r)+C(2_d6.3_r)	3	37.5 (1.4)	0.17	44.7	32.2	41413	484
A(1_d10_r)+C(2_d6.3_r)	3	37.9 (2.0)	0.11	48.7	41.5	37595	461
C(2_d6.3_r)	3	39.6 (1.4)	0.17	40.6	33.4	41286	458
A(2_d6.3_r)+C(2_d6.3_r)	3	40.2 (1.7)	0.06	52.7	37.4	36586	482
A(1_d6.3)+C(1_d6.3_r)**	2	40.9 (1.5)	0.06	41.1	28.2	43838	488
A(1_d6.3)+B(1_d6.3)+C(1_d6.3_r)*	1	38.8 (1.4)	-	38.8	25.2	41571	478
A(2_d6.3)+B(2_d6.3)+C(2_d6.3_r)*	1	36.6 (1,3)	-	49.1	42.8	45750	485

\* : only one specimen was tested in this group  
 \*\*: only two specimens were tested in this group

Table 1 Summary of test results.  $N$  is the number of tested specimens,  $P_{max}$  is the first maximum load,  $\delta_{max}$  is the slip at  $P = P_{max}$ , CoV is the coefficient of variation of  $P_{max}$ ,  $P_{ult}$  is the absolute maximum load,  $P_{\delta=5}$  is the load corresponding to a slip  $\delta = 5$  mm,  $k$  is the stiffness of the joint,  $\rho$  is the density. The moisture content varied in the range 12-13 % for all specimens. The numbers in the table indicate the mean values of test results for each group. (Crocetti, Axelson, & Sartori, 2010)

The results of the test series are summarised in Table 1. By applying reinforcement screws the maximum load  $P_{max}$  was about doubled compared to the non-reinforced group. However, this increase was observed for all reinforced groups of specimens, meaning that the placement and even the number of the screws did not have a significant influence on the result. Furthermore, the scatter (CoV) in the results for  $P_{max}$  was significantly lower for reinforced groups. As for stiffness values  $k$ , a significant increase of about 40 ÷ 60 % was observed for the reinforced groups compared to the non-reinforced group.

The failure mode for the non-reinforced specimens was splitting, with the crack initiated at the end grain. An additional splitting crack could be observed behind the dowel, i.e. opposite of the loaded side of the dowel (Figure 10). In some specimens eventually a shear plug was

formed. The width of the shear plug was usually smaller than the dowel diameter. Failure occurred in a brittle manner.

In the reinforced specimens failure occurred in a more ductile manner. First, a splitting crack was formed at the end grain and then eventually a shear plug was formed after considerable further deformation (Figure 11).

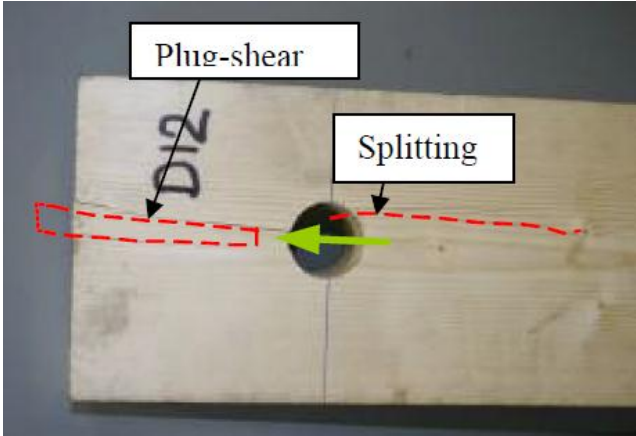


Figure 10 Typical failure mode for non-reinforced specimens. (Crocetti, Axelson, & Sartori, 2010)



Figure 11 Typical failure mode for reinforced specimens. (Crocetti, Axelson, & Sartori, 2010)

## 3 Laboratory Tests

### 3.1 Introduction

To investigate the behaviour of reinforced single large-dowel wood joints full-scale laboratory tests were carried out at the SP Träteck in Borås. 15 glulam specimens with a cross section of 140 mm × 405 mm were tested in load controlled tensile tests. The outer diameter of the employed dowels was 90mm. Each specimen was equipped with an identical design on both ends. For all experiments the load was applied parallel to the grain. The load was increased until failure occurred in one end of the specimen. As the splitting behaviour was of major interest, the end distance of the dowel was set to 3,5 times the diameter of the dowel, which is one half of the minimum end distance recommended in Eurocode 5. The test setup is described more in detail in 3.3.

The test series was divided into five groups of three specimens each. One group was tested without reinforcement, representing a reference for the four other groups which were equipped with different kinds of reinforcement measures. The configurations of the reinforcement measures were determined considering the results of the preliminary small-scale experiments (Crocetti, Axelson, & Sartori, 2010).

Three groups of specimens were reinforced by means of self-tapping screws. The reinforcements of these groups varied in the positioning of the screws and in the angle of the screw axis to the grain (either perpendicular to the grain or inclined at an angle of 45° to the grain). The fourth group of specimens did not involve any self-tapping screws. Instead, the specimens were prestressed laterally (i.e. perpendicular to the grain) using Dywidag rods. Table 2 shows the configurations of reinforcements in the five different groups of specimens. More detailed information about the used reinforcements and their manufacturing can be found in 3.2.



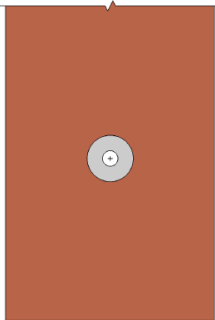
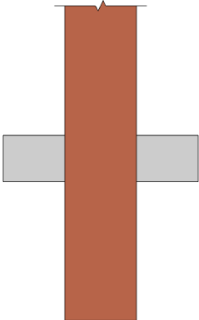
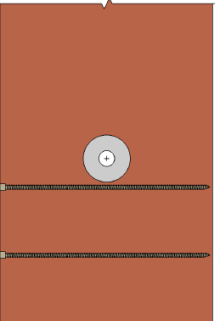
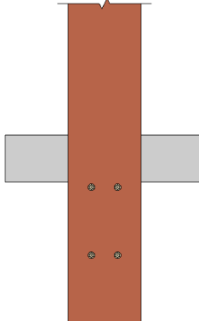
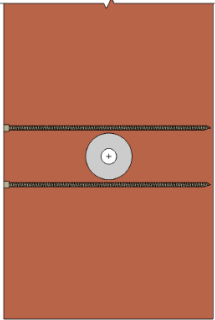
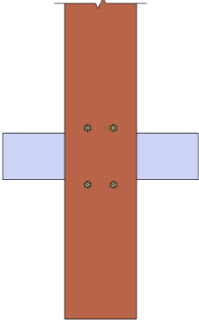
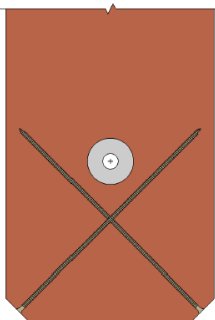
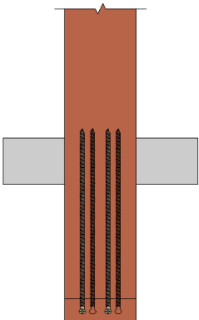
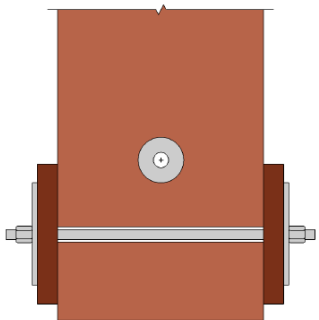
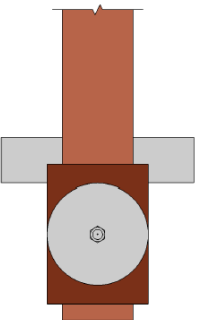
Group name	Type of reinforcement	
“Basic”		
“A2+B2”		
“02+A2”		
“Inclined”		
“Dywidag”		

Table 2 Types of reinforcements.

## 3.2 Specimens and Reinforcements

### 3.2.1 General

15 glulam specimens were used in the test series. The quality of the spruce timber corresponds to the strength class GL30c, with a characteristic tensile strength parallel to the grain of  $f_{t,0,k} = 20$  MPa. The specimens had a cross section of 140 mm  $\times$  405 mm and were 2,30 m in length.



Figure 12 Glulam specimen 140 mm x 405 mm x 2300 mm.

Before testing, average densities of the specimens were derived by weighing the whole specimens. The obtained values of average densities varied in the range of  $437 \text{ kg/m}^3 \leq \rho \leq 486 \text{ kg/m}^3$ . Additionally, densities and moisture contents (MC) were measured after testing on samples taken from the part of the specimen where failure had occurred (i.e. from the shear plug). These values of density varied in the range of  $356 \text{ kg/m}^3 \leq \rho \leq 566 \text{ kg/m}^3$  and the moisture contents were within  $\text{MC} = 8,9 \div 12,4 \%$ .

The dowels used for testing were steel tubes with an outer diameter of 90 mm and an inner diameter of 30 mm, implying a wall thickness of 30 mm. Due to these dimensions, the dowels could be considered rigid and no deformations of the dowels were observed during testing.

Two different types of self-tapping screws were used as reinforcements. These were Konstrux 10 mm  $\times$  400 mm as well as SFS 9 mm  $\times$  500 mm. In order to guide the screws in the right direction, the first 170 mm were pre-drilled with a hole diameter of 4 mm. Since the diameter

of the pre-drilled hole was smaller than 0,6 times the diameter of the screw, this complies with Eurocode 5.

**3.2.2 Specimen Group “Basic”**

The specimens of the group “Basic” were tested without any reinforcements and can be seen as a reference for the reinforced specimens. As in all specimens, the dowel was placed at an end distance of 3,5 times the diameter of the dowel, i.e.  $3,5 \times 90 \text{ mm} = 315 \text{ mm}$ . Manufacturing compromised solely the cutting of the holes for the dowels.

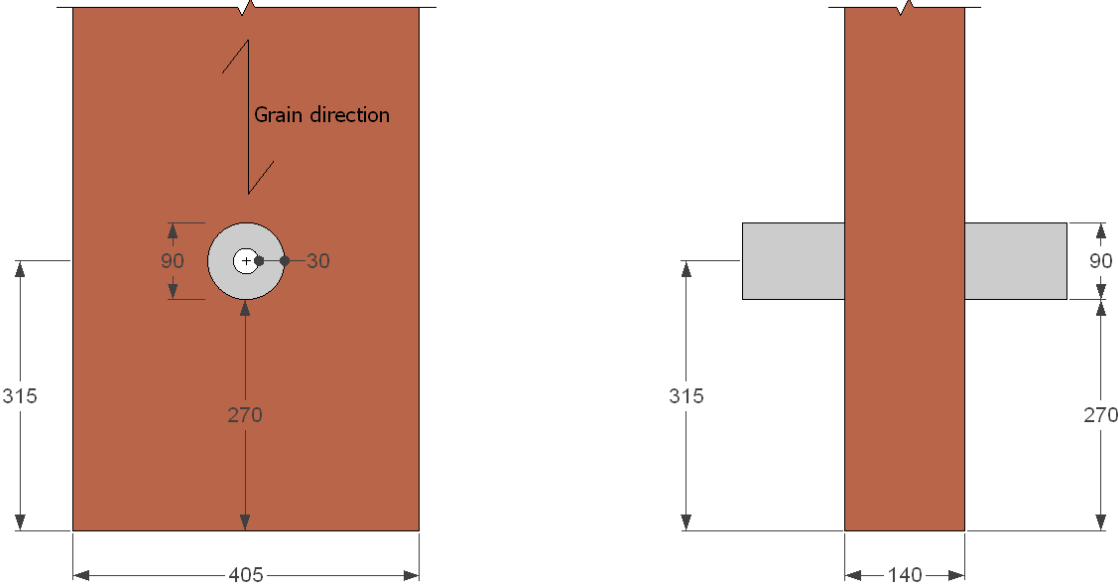


Figure 13 Configuration of specimens in group “Basic”. Units: [mm]

### 3.2.3 Specimen Group “A2+B2”

The specimens in group “A2+B2” were reinforced with self-tapping screws on two levels between the dowel and the loaded end. Two Konstrux 10 mm × 400 mm screws were inserted perpendicularly to the grain at each level. Level A is located only 10 mm from the dowel. The goal was to get the screws as close as possible to the dowel or even allow direct contact between the screws and the dowel. In the process of manufacturing it was observed that in fact many of the screws grazed the dowel while being placed. Besides reinforcing the timber perpendicular to the grain, the screws in level A function as an elastic foundation for the dowel, distributing the load laterally while being subjected to bending. Reinforcement screws placed in contact to the fastener have been studied by Bejtka (2005). Level B is located in the middle between level A and the loaded end. These two screws were primarily intended as lateral tensile reinforcements, compensating the low tensile strength of timber perpendicular to the grain. They are only notably subjected to bending after failure, i.e. after a shear plug has been formed.

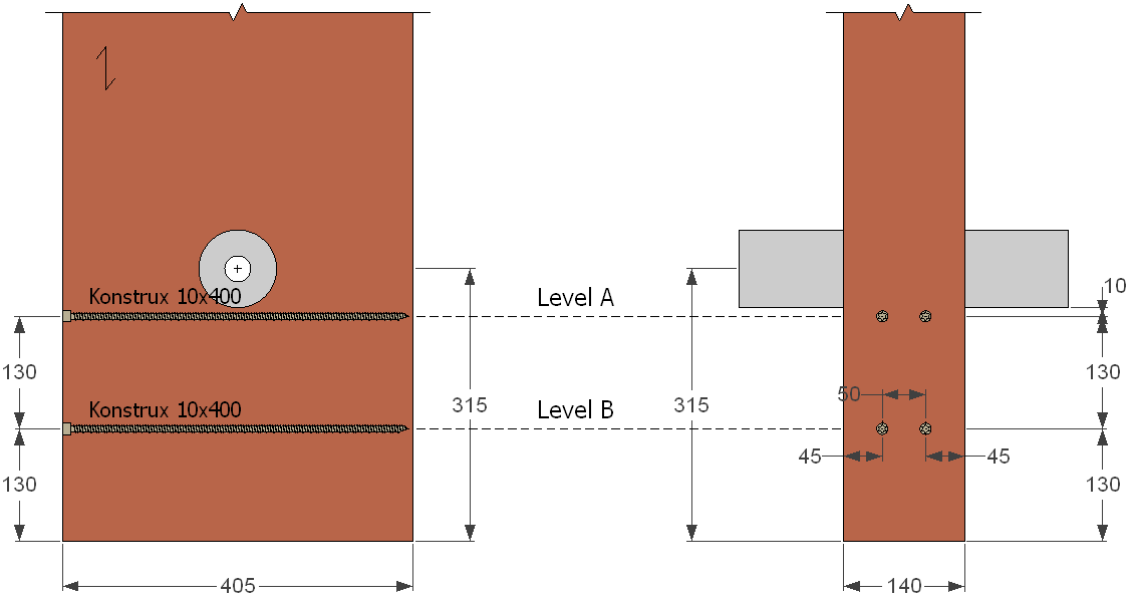


Figure 14 Configuration of specimens in group “A2+B2”. Units: [mm]



*Figure 15 Installing of self-tapping screws.*

### **3.2.4 Specimen Group “02+A2”**

In group “02+A2” again two Konstrux 10 mm × 400 mm screws were placed adjacent to the dowel in level A. Additionally, two SFS 9 mm × 500 mm screws were placed in level 0, which also is located just 10 mm from the dowel, but on the far side of the dowel. This measure was taken based on the results from the small scale tests (Crocetti, Axelson, & Sartori, 2010), where splitting was observed not only on the loaded side of the dowel, but also on the far side. Screws in level 0 are not directly loaded by the dowel and thus not subjected to bending. They function solely as a lateral reinforcement of the timber.

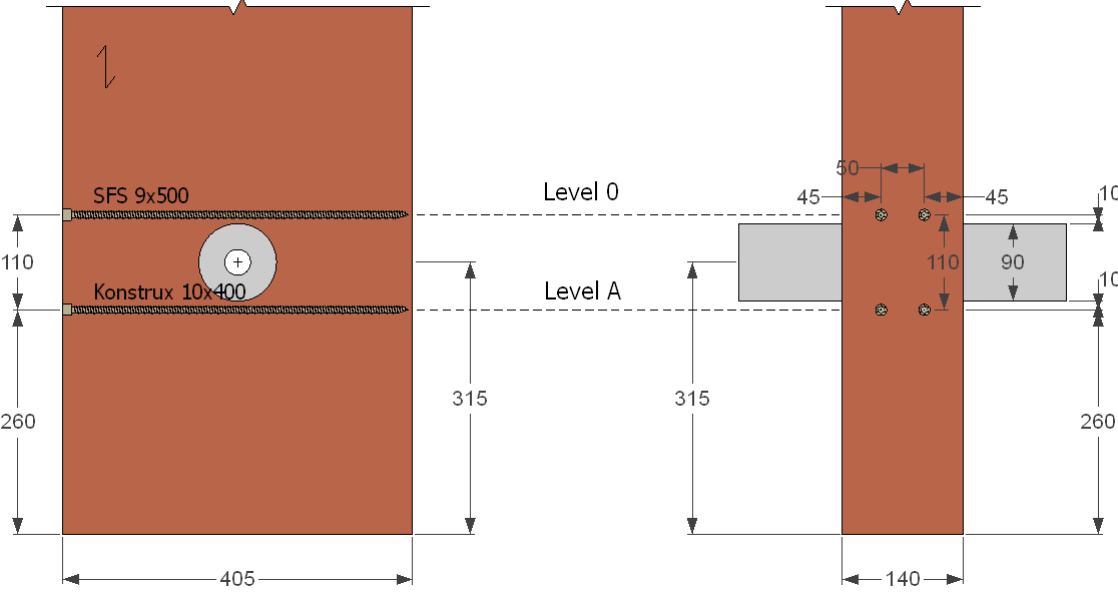


Figure 16 Configuration of specimens in group “02+A2”. Units: [mm]

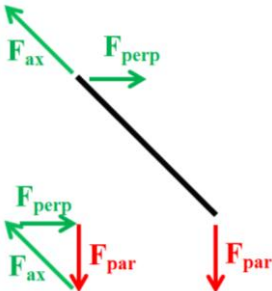
Since the screws used in level 0 were longer than the height of the specimens, they appeared on the far side of the specimen when being installed. It was observed that the self-tapping screws often deviated from their designated position (Figure 17), despite being guided by the pre-drilled hole on the first 170 mm. However, this was expected as it could not be assumed that self-tapping screws would go perfectly straight over a distance of over 400 mm.



Figure 17 Self-tapping screws in level 0 (specimen no. 7).

**3.2.5 Specimen Group “Inclined”**

In group “Inclined” four SFS 9 mm × 500 mm screws were used to reinforce the specimen. Instead of being placed perpendicularly they were installed at an angle of 45° to the grain. For a load parallel to the grain, inclined screws will predominantly be subjected to tensile forces, as opposed to bending in screws positioned perpendicular to the grain. The axial force in the screws leads to a force component perpendicular to the grain, compressing the timber and thus counteracting the timbers tendency to split (Figure 18).



*Figure 18 Force components in inclined screws.*

For installing the screws the corners of the specimen were cut off and the screws were screwed in beginning from the loaded end towards and past the dowel. Again the screws did not perfectly follow their designated path and the tips of some screws did even appear on the side of the specimen (Figure 19). As the tips of the screws were located way outside of the failure area, this was not expected to cause negative effects on the performance of the reinforcement, which was confirmed by the test results.



*Figure 19 Screw tip appearing on the side (specimen no. 10).*

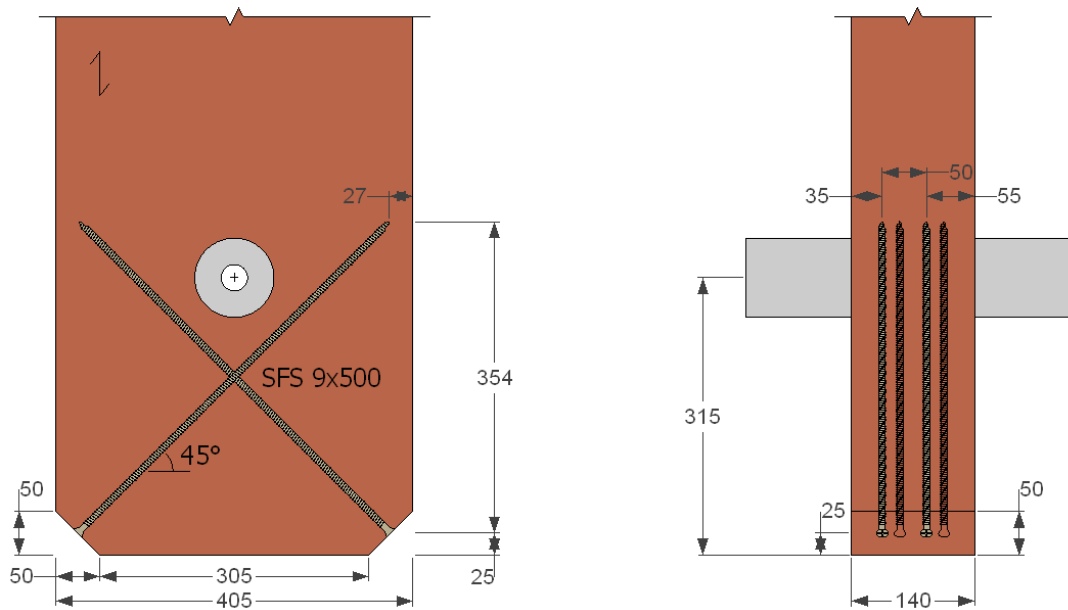


Figure 20 Configuration of specimens in group “Inclined”. Units: [mm]

### 3.2.6 Specimen Group “Dywidag”

For the specimens in group “Dywidag” a different approach was used for reinforcing compared to the other groups. Instead of reinforcing the timber with self-tapping screws the area between the dowel and the loaded end was prestressed laterally using a Dywidag rod. Thereby the timber was compressed perpendicular to the grain. As observed in the small scale tests (Crocetti, Axelson, & Sartori, 2010), the timber tends to split for increasing loads and the ultimate failure mode is a shear plug. Compressing the timber perpendicular to the grain counteracts the splitting tendency and increases the shear strength along the grain, thus impeding the shear plug to form. The Dywidag rod itself was not intended to contribute to the reinforcement (e.g. by its bending strength). Its sole purpose was to apply the prestressing force to the timber. Therefore the Dywidag rod ( $d = 15 \text{ mm}$ ) was led in a 30 mm hole to avoid the rod getting into contact with the timber.

For the load transmission from the Dywidag rod to the timber a 40 mm thick hard wood plate was used (Figure 21). The hard wood plate was 275 mm in length and distributed the prestressing force on the area between the dowel and the loaded end.



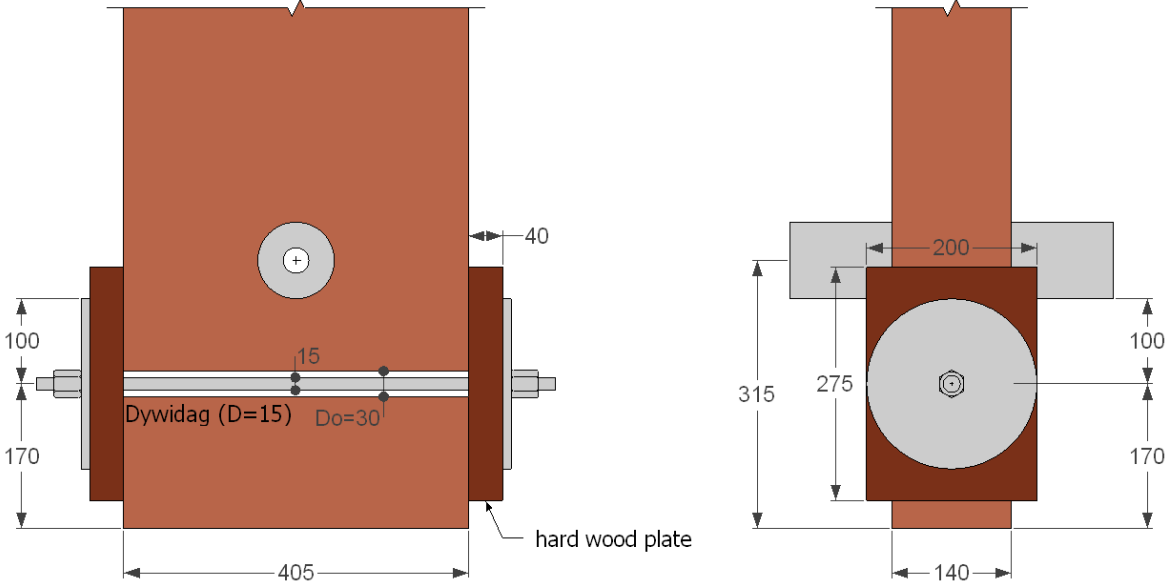


Figure 21 Configuration of specimens in group "Dywidag". Units: [mm]

The prestressing force was applied in two steps to reduce the loss of prestress due to creep deformations. The limiting factor for prestressing was the tensile strength of the Dywidag rod. It allowed a maximum load of about 160 kN, but about 20 % of were lost immediately in the process of load transfer from the pretension jack to the nut. The second prestressing was conducted immediately before the test was started and the force in the Dywidag rods was measured continuously during the test. Given the conditions mentioned above, a contact prestress between the hard wood plate and the timber of  $2,9 \div 3,3$  MPa could be applied. The first specimen (no. 13) that was tested was prestressed at a slightly lower level than the other two. Table 3 shows the levels of prestress in the specimens before testing.

Specimen no.	Prestress [MPa]	
	End I	End II
13	3,0	2,9
14	3,2	3,2
15	3,2	3,3

Table 3 Prestress in Dywidag specimens.



Figure 22 Prestressing.

Specimen no.	initial prestressing	second prestressing	Total	
	$\Delta_1$ [mm]	$\Delta_2$ [mm]	$\Delta_{tot}$ [mm]	$\varepsilon$ [%]
14	9,8	3,6	13,3	3,3
15	13,6	1,3	14,9	3,7

Table 4 Deformations and strain due to prestressing.

A prestress level of over 3 MPa is high, considering that Eurocode 5 sets the characteristic compression strength of glulam GL30c perpendicular to the grain at  $f_{c,90,k} = 2,5$  MPa. Exceeding the compression strength according to Eurocode leads to a substantial increase in deformation. For specimens number 14 and 15, the deformations due to prestressing were measured at one end of the specimen each. Figure 23 shows the deformations resulting from the first application of prestressing force. It can be seen that the deformation rate increases significantly for higher stresses. The initial prestressing caused a deformation of 9,8 mm in specimen 14 and 13,6 mm in specimen 15. Additional deformations of 3,6 mm and 1,3 mm respectively were caused by the second prestressing. The total deformations of 13,3 mm in specimen 14 imply a strain of 3,3 %, for specimen 15 total deformations are 14,9 mm implying a strain of 3,7 %.

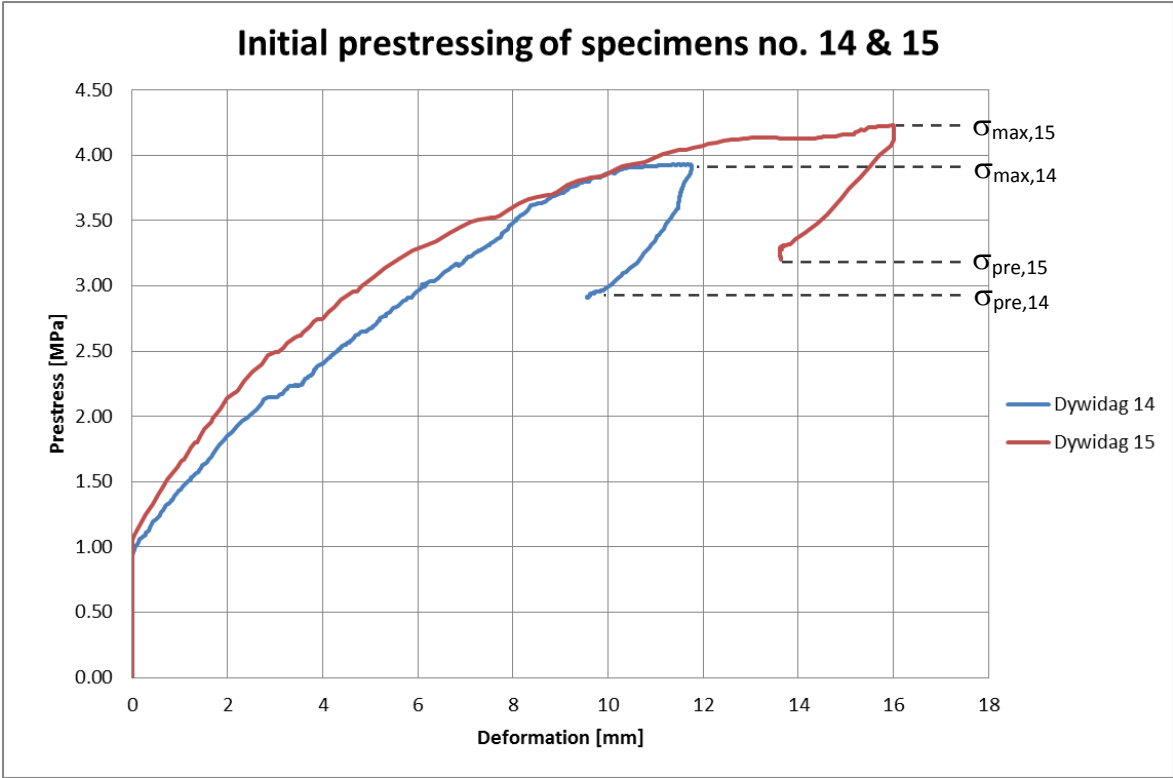


Figure 23 Initial Prestressing of specimens no. 14 & 15.

### 3.3 Test Setup

#### 3.3.1 Setup and Loading Procedure

The tests were carried out as quasi-static tensile tests. The specimens were placed horizontally and the load was applied in line with the axis of the specimen by a hydraulic cylinder. Each

specimen was equipped with an identical design of a single dowel connection on both ends. The connections between the dowels and the hydraulic device were constructed with an assembly of Dywidag rods and square steel profiles (Figure 25). Before starting to apply the load, the specimens were resting on supports in a position where the axis of the specimen was marginally lower than the axis of the testing machine. Thereby it was ensured that the specimen was lifted from the supports when load was applied, preventing influences on the test results by supporting elements.

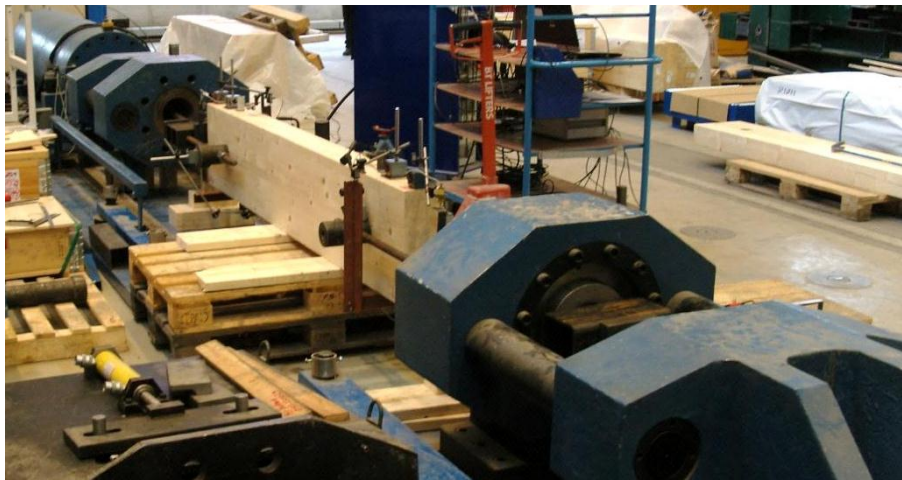


*Figure 24 Test setup.*

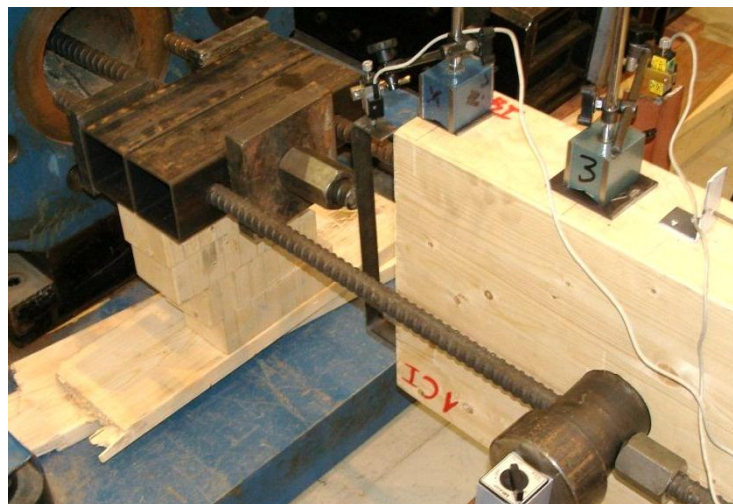


*Figure 25 Load transfer from dowel to machine.*

The tests were performed under load control, following the loading procedure suggested by the European Standard EN 26 891 for timber structures. The load was increased until failure was reached in one end. Figure 26 shows the loading procedure as a function of the estimated maximum load ( $F_{est}$ ). The approximate maximum loads had to be estimated in order to scale

the loading curve for each test. Table 5 lists the estimated maximum loads for all groups of specimens. In group “02+A2” the estimated maximum load was adjusted after the first of three tests, in group “Dywidag”  $F_{est}$  was adjusted after having performed two out of three tests.

Group	$F_{est}$ (/adjusted)
Basic	130 kN
A2+B2	220 kN
02+A2	220 / 175 kN
Inclined	200 kN
Dywidag	275 / 300 kN

*Table 5 Estimated maximum loads.*

The loading procedure consists of the following steps:

- Increase load to  $0,4F_{est}$
- Maintain load for 30 seconds
- Reduce load to  $0,1F_{est}$
- Maintain load for 30 seconds
- Increase load until failure.

Below  $0,7F_{est}$  a constant loading rate of  $0,2F_{est}$  per minute is used. Above  $0,7F_{est}$ , the loading rate is adjusted to  $0,075F_{est}$  so that the ultimate load is reached in about 4 minutes additional testing time. By following this procedure the total testing time adds up 11,5 minutes.

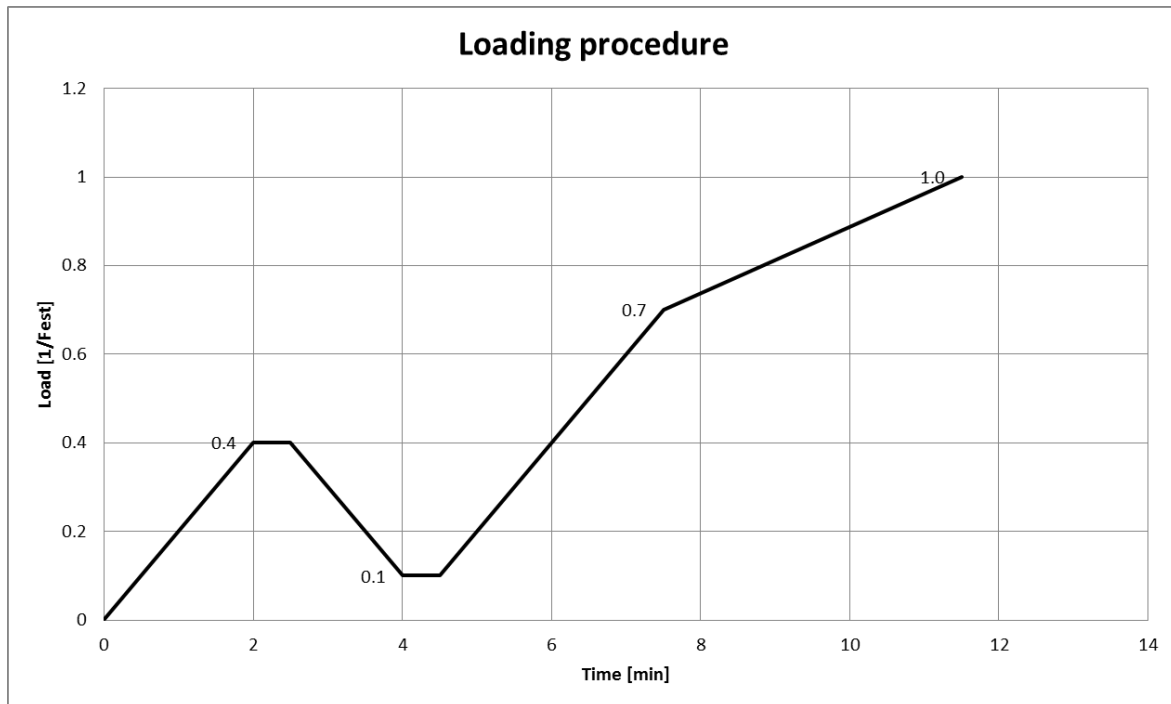


Figure 26 Loading procedure.

### 3.3.2 Measurements

During testing the dowel slip in the connection as well as lateral deformations in the specimen were continuously measured. To capture possible rotations of the dowel two sensors were used to measure the slip. The sensors were placed on the dowel on each side of the specimen, measuring the relative deformation of the dowel towards the timber at the edge of the specimen in the same cross section. The lateral deformations were measured in two different positions between the dowel and the loaded end. One sensor was installed 5 cm from the dowel, the other sensor was placed at the loaded end. The lateral deformations were measured from edge to edge, i.e. the recorded values were the total deformations occurring over the height of the specimen. Due to the dimensions of the prestressing elements in group “Dywidag”, the lateral deformations in those specimens could only be measured at the loaded end. To continuously measure the prestressing force in group “Dywidag”, load cells were installed.

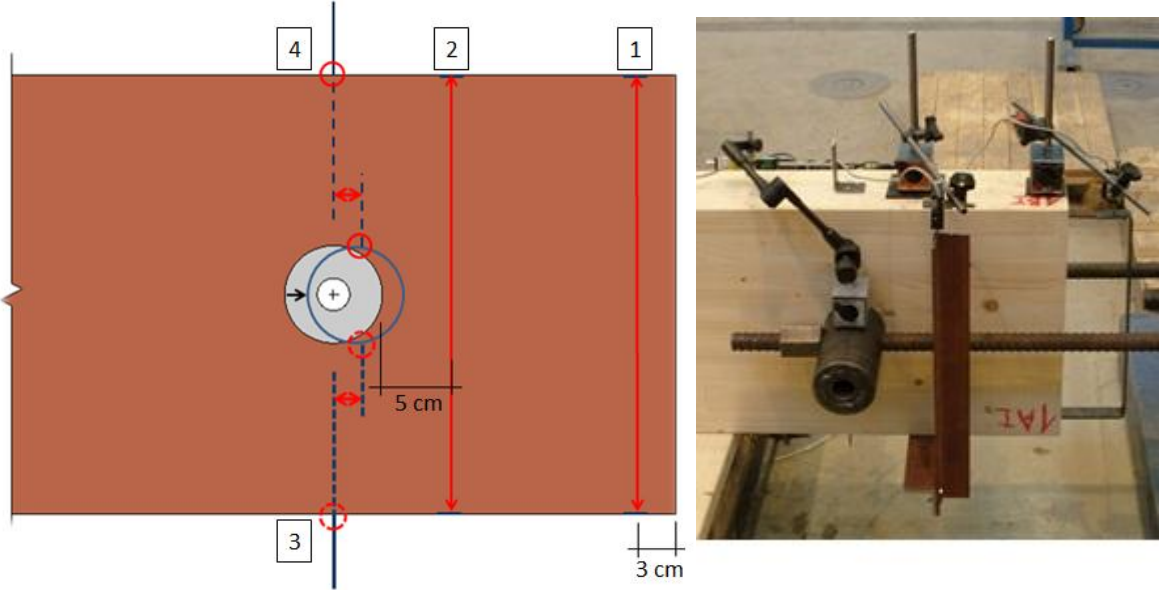


Figure 27 Measurements. 1 & 2: lateral deformation; 3 & 4: dowel slip.

## 4 Results

### 4.1 Annotations

In chapters 4.2 - 0 the results of the conducted tests are presented separately for each group of specimens. A summary of the obtained results can be found in 4.7.

The fact that the tests were performed under load control had an impact on the collected data. The load controlled procedure was adopted because the employed testing machine did not allow displacement control. It implicated that the testing machine rapidly increased the deformation when the resistance of the connection dropped after the maximum load had been reached, trying to keep up the designated load level. This resulted in a rather violent process of failure, shaking the whole specimen and sometimes even causing the sensors to fall off. Therefore, the load-slip curves could only be recorded consistently until the maximum load was reached and consequently the diagrams in the following chapters display the deformations only to the point where failure occurred. Nevertheless, the applied load was recorded even after failure, allowing to determine a residual strength of the connection.

As described in 3.3, all specimens were equipped with an identical design on both ends and the load was increased until failure was reached in one end. This procedure implies that the actual bearing capacity could only be determined for half of the prepared connections. The analysis of the tests will mainly focus on the connections where failure was reached. The diagrams shown in 4.2 - 0 always show the behaviour of the connections where failure occurred. However, valuable data could also be derived from the connections which did not fail.

As for bearing capacity, the information that was taken from the connections that stayed intact was that their bearing capacity was at least equal to the corresponding bearing capacity of the failed connection on the other end of the specimen. The fact that in each test only one of the connections failed at the measured bearing capacity shows that the other connection in the same specimen actually did have a higher bearing capacity. However, since there is no indication of how much higher the bearing capacity of the intact connection could be, it was



assumed that it was only infinitesimally higher i.e. equal to the measured value in the failed connection. This assumption is conservative, as it does not raise the mean value of the measured bearing capacities, even though the tests had shown that that the actual mean value had to be at least somewhat higher. On the other hand, using these conservative values does have a positive effect on the calculated coefficient of variation (CoV) as it doubles the sample size.

Values of stiffness could be gathered from all connections, regardless whether failure was reached or not. The stiffness  $k^{slip}$  of the connections was determined as the rate of dowel slip in load direction between  $0,4F_{est}$  and  $0,7F_{est}$ , with  $F_{est}$  standing for the estimated maximum load (see 3.3.1).

To compare lateral deformations in the connections the value  $k^{lat}$  [kN/mm] is introduced. It is not an actual stiffness value, as it connects the load applied on the dowel (parallel to the grain) with the lateral deformation occurring at the loaded end of the connection (perpendicular to the grain).

Furthermore, splitting of the timber could be observed also in some connections which did not reach failure. This information was included in the analysis as well.

Furthermore, the loads  $F_{split}$  when splitting occurred were detected. In the connections where splitting prior to failure was observed,  $F_{split}$  could be detected directly. For connections where no splitting prior to failure was observed it is assumed that the ultimate failure (shear plug) was initiated by splitting. This means that in these connections the splitting load  $F_{split}$  is equal to the bearing capacity  $F_{max}$ .

## 4.2 Results Group “Basic”

Figure 29 shows the load-slip behaviour for the three connections in the non-reinforced group “Basic” where failure was reached, whereas Figure 30 shows the measured lateral deformations. The average bearing capacity was  $F_{max} = 134$  kN with a coefficient of variation of  $CoV = 4,1$  %. The corresponding mean slip of the connection at  $F_{max}$  was  $\delta_{max} = 0,48$  mm. After failure the resistance of the connections immediately dropped to values close to zero, so it can be stated that there was no residual strength to speak of.

In specimens 1 and 2 splitting of the timber was observed prior to failure at loads of 110 kN and 80 kN respectively. The sudden increase in lateral deformation caused by splitting can be verified in Figure 30. Splitting also caused sudden increases in dowel slip as can be seen in Figure 29. It was observed that splitting started at the end of the specimens and not at near the dowels (Figure 28). For specimen 3 splitting was not observed before failure at  $F_{max} = 135$  kN. The deviation in the load-slip curve in Figure 29 is caused by splitting in the other connection on the opposite end of the specimen, which shook the whole specimen. Figure 30 shows no sign of premature splitting for specimen 3 as the curve is approximately linear until failure. Furthermore, Figure 30 displays that the lateral deformations were significantly larger at the end than near the dowel.

The ultimate failure mode was a shear plug for all three specimens and failure occurred in a brittle manner. Figure 29 shows a slightly non-linear behaviour before maximum load only for specimen 2, specimen 1 and 2 show a linear behaviour until failure. The width of the shear plug was somewhat smaller than the dowel diameter for all three specimens. Figure 31 shows the shear plug in specimen 2. It can also be seen that the timber was split over a long distance ( $> 1$  m) on the unloaded side of the dowel. This occurred in all three tests due to the wedging effect of the dowel at large deformations after failure. In the specimens where splitting had occurred prior to failure (specimens 1 and 2) the initial cracks formed a shear plane of the plug (see Figure 28 and Figure 31).

Considering the data of all six connections involved in this test group – including the connections where failure was not reached - the following behaviour was observed for loads below bearing capacity:

In five out of six connections splitting was observed (including assumed splitting at  $F_{\max}$  in specimen 3). The splitting loads  $F_{\text{split}}$  were between 80 kN and 135 kN with an average of 105 kN. The lateral deformations at splitting were within the range of 0,78 mm ÷ 1,40 mm, which corresponds to an average lateral strain of 1,93 ÷ 3,46 ‰ over the height of the specimen. The lateral deformations at the loaded end occurred at a mean lateral stiffness of  $k^{\text{lat}} = 93$  kN/mm (CoV = 21,2 ‰). Lateral deformations near the dowel were only marginal.

For the load-slip behaviour of the dowel connections the mean stiffness was calculated to  $k^{\text{slip}} = 308$  kN/mm (CoV = 15,2 ‰).



*Figure 28 Splitting in Specimen 2.*

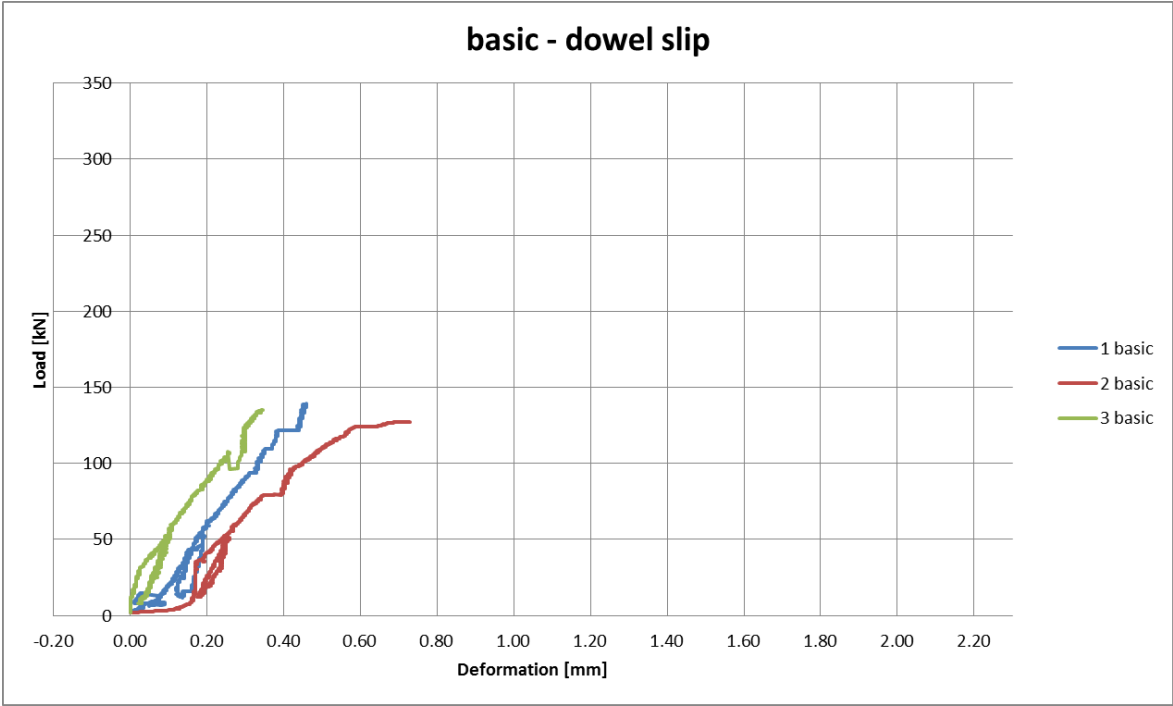


Figure 29 Load-slip behaviour in group "Basic".

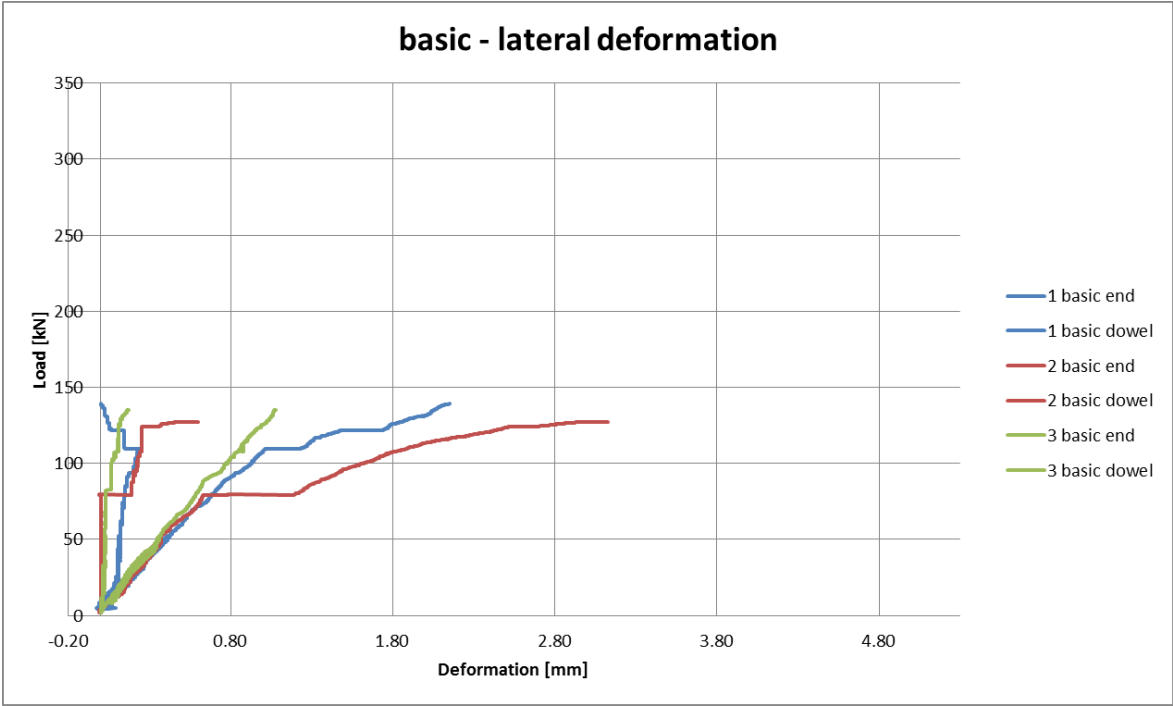


Figure 30 Load-lateral deformation behaviour in group "Basic".



Figure 31 Shear plug in specimen 2.

### 4.3 Results Group “A2+B2”

The connections in group “A2+B2” were reinforced with self-tapping screws at the loaded end as well as close to the dowel (see 3.2.3). Figure 33 shows the load-slip behaviour for the three connections in group “A2+B2” where failure was reached, Figure 34 shows the measured lateral deformations. The average bearing capacity was  $F_{max} = 237$  kN with a coefficient of variation of  $CoV = 8,4$  %. The corresponding mean slip of the connection at  $F_{max}$  was  $\delta_{max} = 1,06$  mm. After failure an average residual strength of  $F_{res} = 183$  kN (77 %  $F_{max}$ ) was measured.

In specimen 5 splitting occurred prior to failure at a load of 180 kN. The process of splitting in specimen 5 is displayed in Figure 34. It shows that splitting was initiated at the loaded end of the connection, as there is a clear unsteadiness in the lateral deformations measured at the end but none near the dowel. In specimens 4 and 6 no splitting occurred before the maximum load was reached, which is reflected by the linear course of lateral deformations. For all three specimens, Figure 34 shows the significant difference between the lateral deformations at the end and near the dowel. While deformations at the end correlate with the applied load, almost no deformations were measured near the dowel. For specimens 4 and 5 the lateral deformation near the dowel was even slightly negative, meaning the cross section was marginally compressed rather than expanded.

The ultimate failure mode was a shear plug for all three specimens. The connections showed a more ductile behaviour than the non-reinforced connections of group “Basic” as the load-slip curves in Figure 33 show an increased deformation rate before the bearing capacity is

reached. The width of the shear plug was smaller than the dowel diameter in specimen 6, in specimens 4 and 5 it was about equal with the dowel diameter. Figure 35 shows the shear plug in specimen 5. The initial split was only partially identical with one shear plane of the plug (see Figure 32 and Figure 35).

Considering the data of all six connections involved in this test group – including the connections where failure was not reached - the following behaviour was observed for loads below bearing capacity:

In four out of six connections splitting was observed. Splitting occurred prior to failure in two of these connections and right at failure in the other two. The splitting loads  $F_{\text{split}}$  were between 155 kN and 251 kN with an average of 199 kN. The lateral deformations at splitting were within the range of 1,45 mm ÷ 2,12 mm, which corresponds to an average lateral strain of 3,58 ÷ 5,23 ‰ over the height of the specimen. The lateral deformations at the loaded end occurred at a mean lateral stiffness of  $k^{\text{lat}} = 115$  kN/mm (CoV = 10,8 %). Lateral deformations near the dowel were only marginal.

For the load-slip behaviour of the dowel connection the stiffness was calculated to  $k^{\text{slip}} = 336$  kN/mm (CoV = 8,7 %).



*Figure 32 Splitting in specimen 5.*

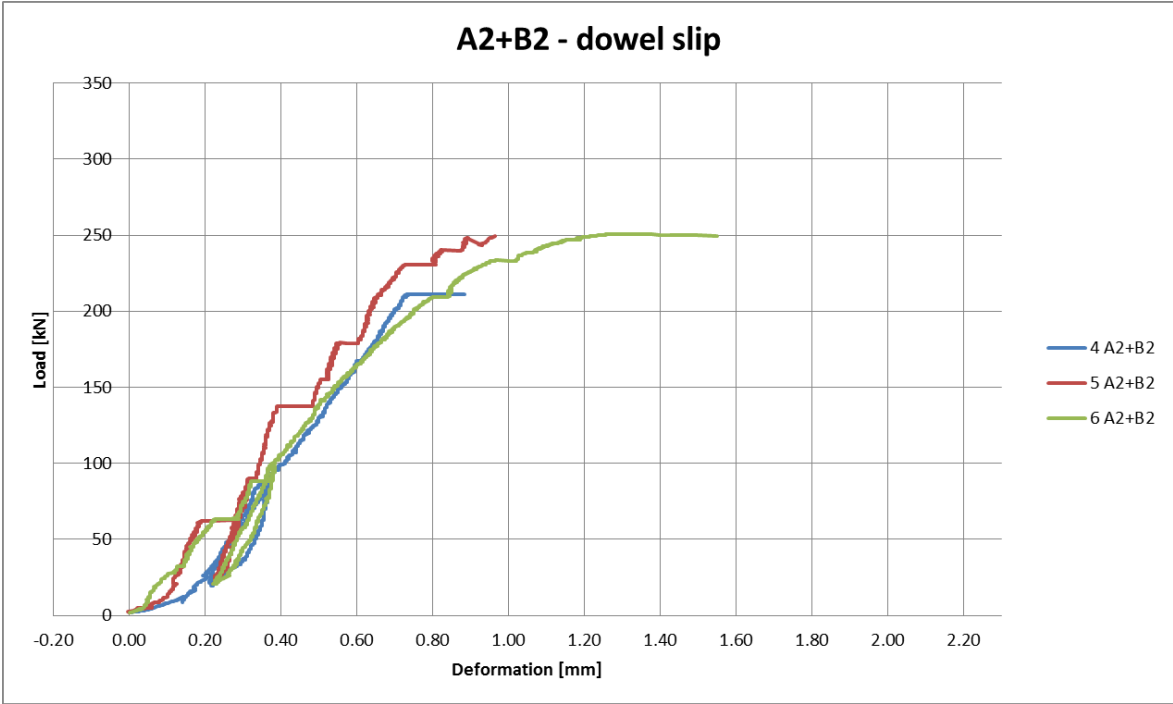


Figure 33 Load-slip behaviour in group "A2+B2".

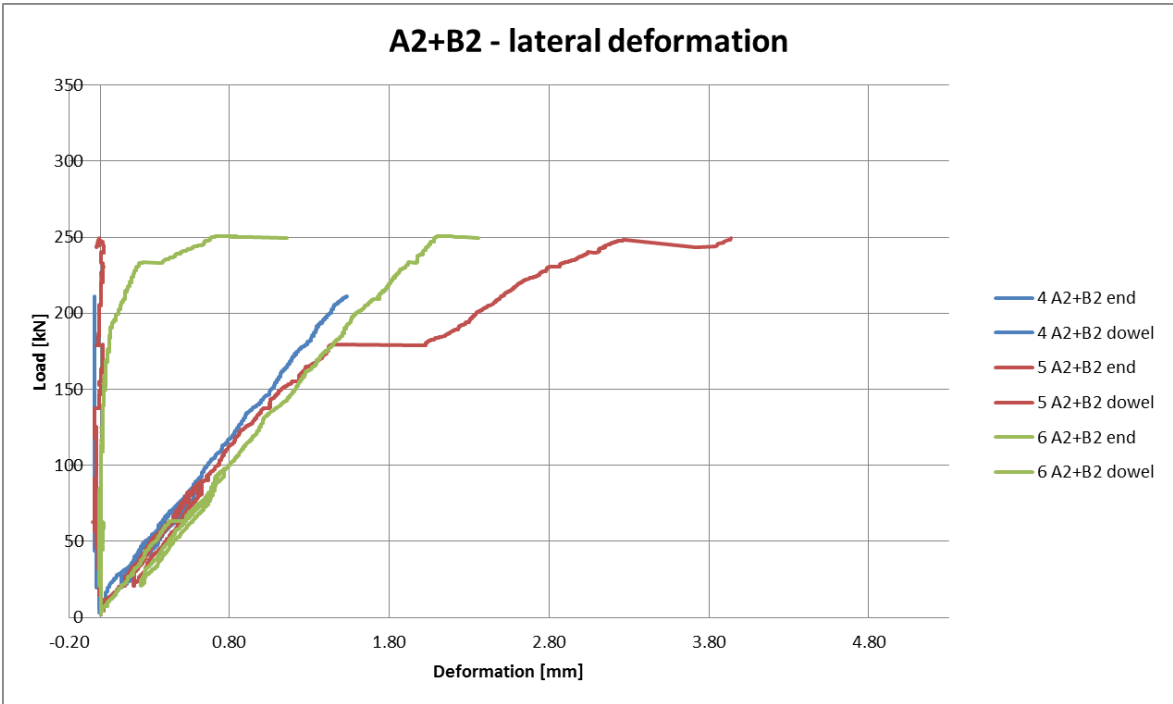


Figure 34 Load-lateral deformation behaviour in group "A2+B2".

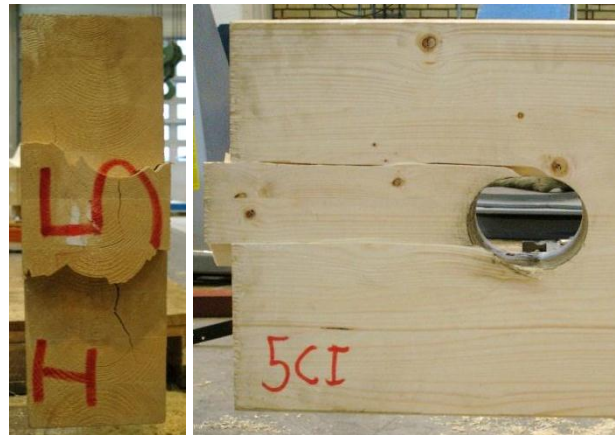


Figure 35 Shear plug in specimen 5.

#### 4.4 Results Group “02+A2”

In group “02+A2” the connections were reinforced with self-tapping screws on both sides of the dowel (see 3.2.4). Figure 37 shows the load-slip behaviour for the three connections in group “02+A2” where failure was reached, Figure 38 shows the measured lateral deformations. The average bearing capacity was  $F_{max} = 187$  kN with a coefficient of variation of  $CoV = 8,9$  %. The corresponding mean slip of the connection at  $F_{max}$  was  $\delta_{max} = 1,24$  mm. After failure an average residual strength of  $F_{res} = 112$  kN (60 %  $F_{max}$ ) was measured.

In specimen 8 and 9 splitting occurred at loads of 163 kN and 142 kN before the maximum load was reached. Specimen 7 showed no sign of splitting before failure. Splitting in specimen 8 and 9 happened very abrupt and violently. As can be seen in Figure 38 the sensors for measuring lateral deformations in specimen 8 fell off in the process of splitting. For specimen 9 an abrupt increase in lateral deformations of several millimetres was measured after splitting. This is confirmed by Figure 36 which shows that the fracture opening at the loaded end indeed was in that scale and that the timber was split over the whole length between the dowel and the end. The load-slip curve for specimen 9 shows also an abrupt deviation due to splitting. Again, Figure 38 shows the significant difference between the lateral deformation rates at the loaded end and at the dowel.

The ultimate failure mode was a shear plug for all three connections. The width of the shear plug was about equal to the dowel diameter or marginally smaller in all cases. In specimen 9



the initial split formed a shear plane of the plug. In specimen 8 however, the initial crack lied within the plug and two different shear planes appeared to form the plug (Figure 39). Figure 37 shows a somewhat ductile behaviour for specimen 8 and 9 before reaching the maximum load. Specimen 7 – where no splitting prior to failure had occurred – did not show any sign of ductility as shear failure occurred suddenly without a foregoing increase in the slip rate.

Considering the data of all six connections involved in this test group – including the connections where failure was not reached - the following behaviour was observed for loads below bearing capacity:

In four out of six connections splitting was observed. Splitting occurred prior to failure in three of these connections and right at failure in one connection. The splitting loads  $F_{split}$  were between 142 kN and 193 kN with an average of 168 kN. The lateral deformations at splitting were within the range of 1,43 mm ÷ 2,15 mm, which corresponds to an average lateral strain of 3,53 ÷ 5,31 ‰ over the height of the specimen. The lateral deformations at the loaded end occurred at a mean lateral stiffness of  $k^{lat} = 95$  kN/mm (CoV = 21,3 %). Lateral deformations near the dowel were only marginal.

For the load-slip behaviour of the dowel connection the stiffness was calculated to  $k^{slip} = 360$  kN/mm (CoV = 11,4 %).



Figure 36 Splitting in specimen 9.

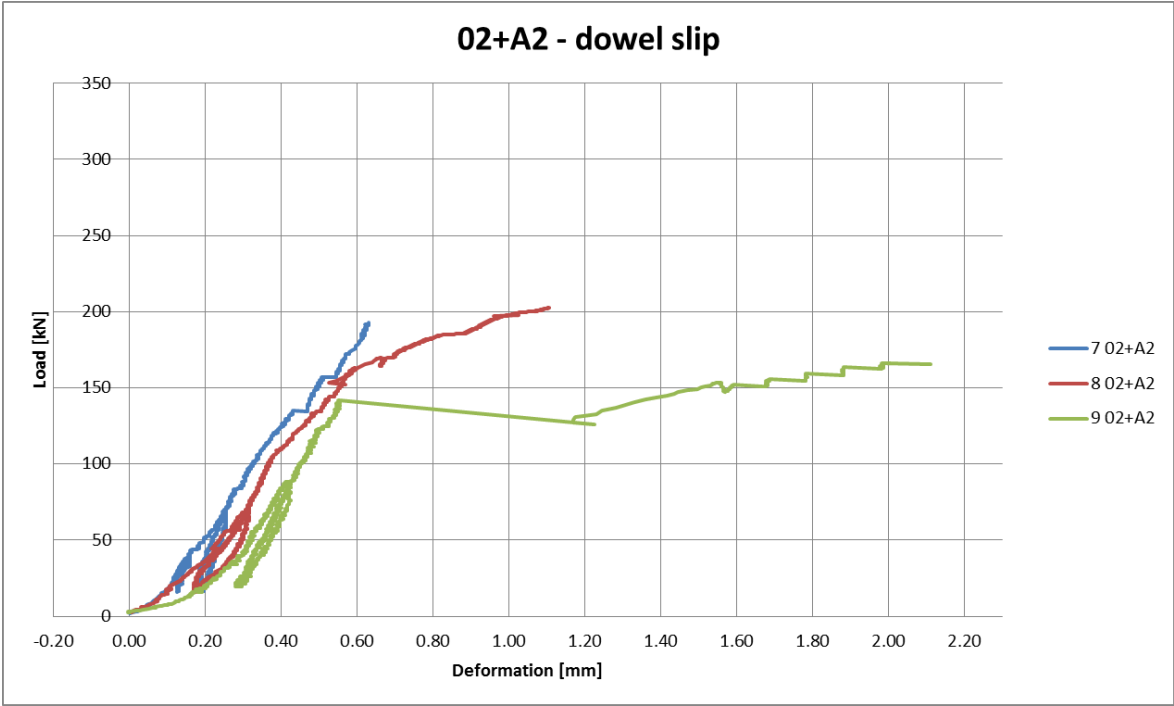


Figure 37 Load-slip behaviour in group "02+A2".

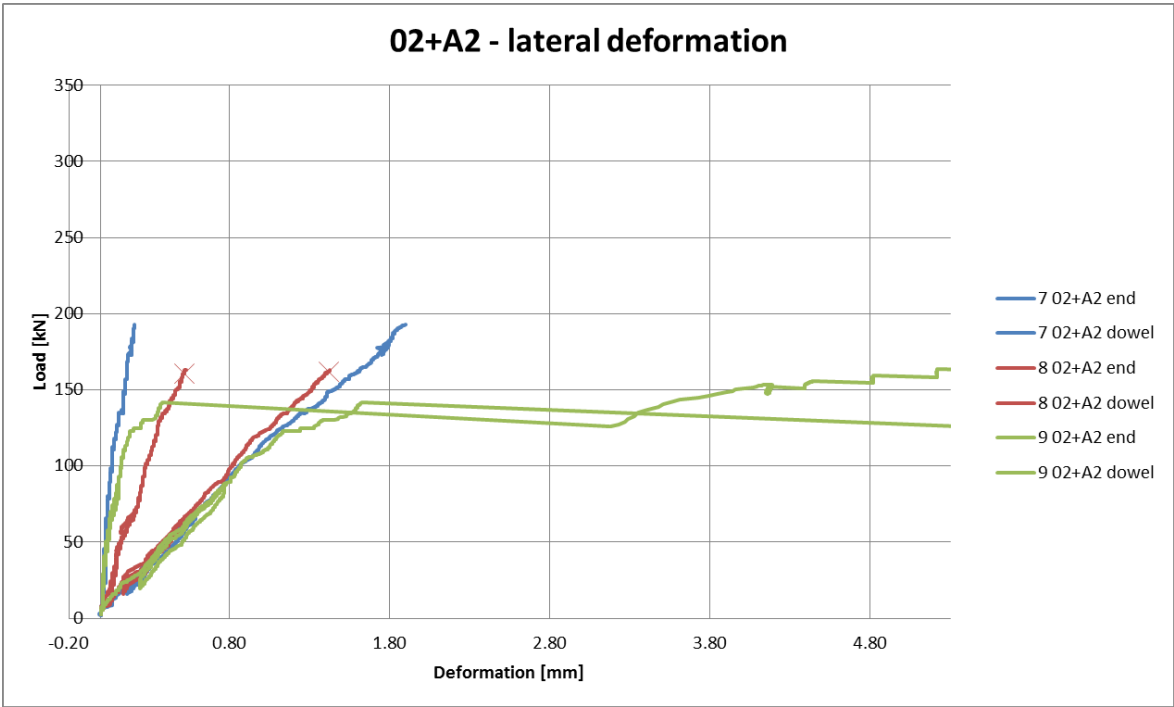


Figure 38 Load-lateral deformation behaviour in group "02+A2".



Figure 39 Shear plug in specimen 8.

#### 4.5 Results Group “Inclined”

In group “Inclined” the connections were reinforced with self-tapping screws inserted crosswise at an angle of  $45^\circ$  to the grain (see 3.2.5). Figure 41 shows the load-slip behaviour for the three connections in group “Inclined” where failure was reached, Figure 42 shows the measured lateral deformations. The average bearing capacity was  $F_{max} = 229$  kN with a coefficient of variation of  $CoV = 8,6$  %. The corresponding mean slip of the connection at  $F_{max}$  was  $\delta_{max} = 1,28$  mm. After failure an average residual strength of  $F_{res} = 151$  kN (66 %  $F_{max}$ ) was measured.

In specimen 10 splitting occurred at a load of 133kN before the maximum load was reached, as can be seen in Figure 42. After the initial split the lateral deformation curve is non-linear with several sudden increases in deformation at the end. The deformations near the dowel also show a non-linear behaviour and are even alternating between compression and extension. However, this result could have been influenced by shaking of the specimen after splitting, so it has to be regarded with reservation. In specimens 11 and 12 splitting was not observed until failure, which is confirmed by approximately linear curves in Figure 42. Lateral deformations near the dowel were significantly smaller than at the end. For specimen 11 negative lateral deformations (i.e. compression) were measured near the dowel.

The ultimate failure mode was shear plug for all three connections (Figure 40). The width of the shear plug was about equal to the dowel in all cases. The initial split in specimen 10

formed a shear plane in the plug. Figure 41 shows signs of ductile behaviour for specimens 10 and 12, whereas specimen 11 shows almost linear load-slip behaviour until failure.

Considering the data of all six connections involved in this test group – including the connections where failure was not reached - the following behaviour was observed for loads below bearing capacity:

Splitting was observed in three out of six connections. Splitting occurred prior to failure in one of these connections and right at failure in two connections. The splitting loads  $F_{split}$  were between 133 kN and 252 kN with an average of 204 kN. The lateral deformations at splitting were within the range of 1,22 mm ÷ 2,01 mm, which corresponds to an average lateral strain of 3,01 ÷ 4,96 ‰ over the height of the specimen. The lateral deformations at the loaded end occurred at a mean lateral stiffness of  $k^{lat} = 121$  kN/mm (CoV = 17,2 %). Lateral deformations near the dowel were only marginal.

For the load-slip behaviour of the dowel connection the stiffness was calculated to  $k^{split} = 336$  kN/mm (CoV = 15,2 %).



Figure 40 Shear plug in specimen 11.

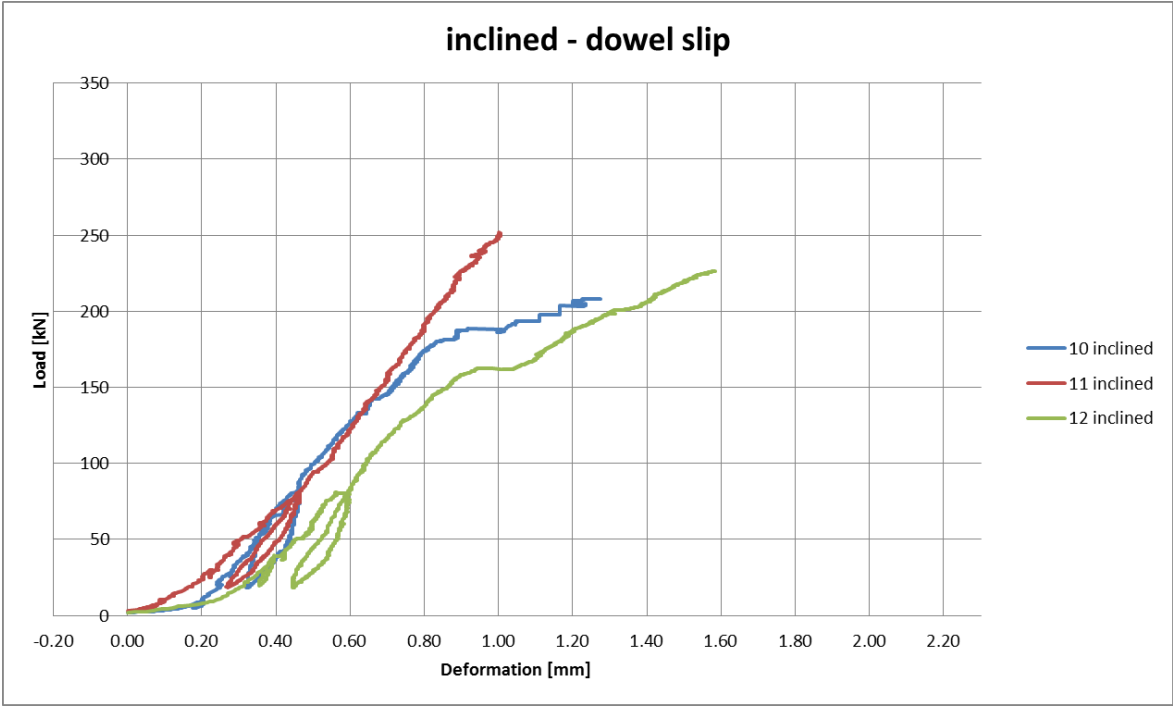


Figure 41 Load-slip behaviour in group "Inclined".

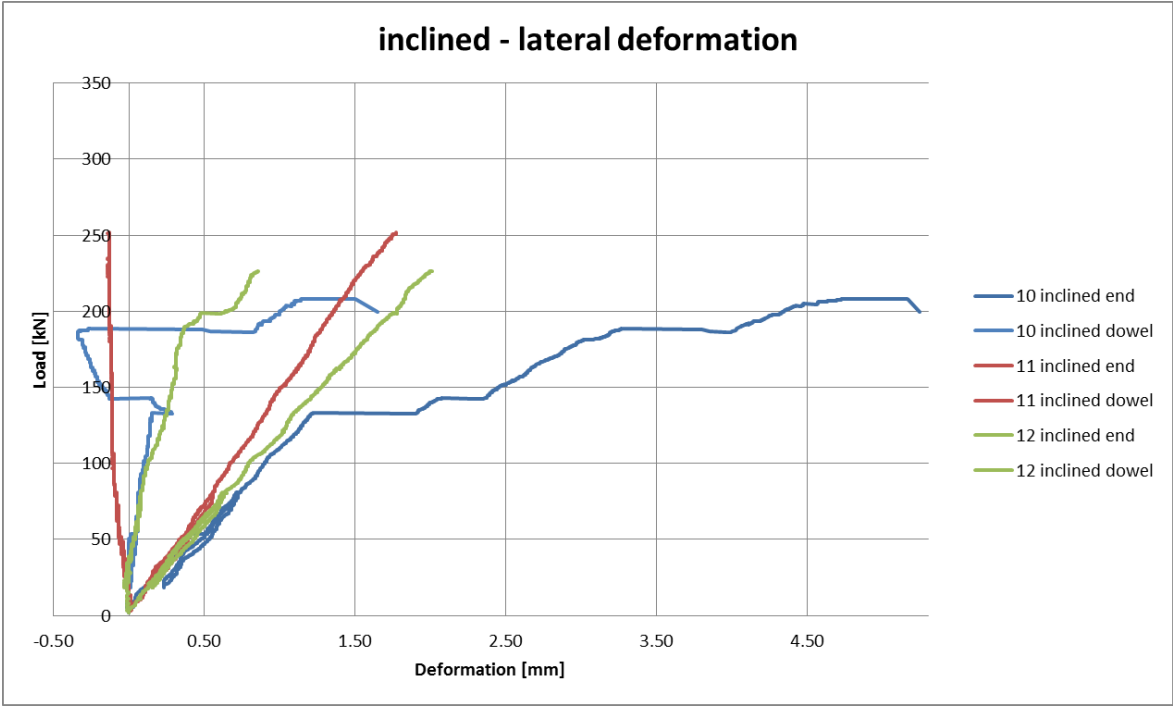


Figure 42 Load-lateral deformation behaviour in group "Inclined".

## 4.6 Results Group “Dywidag”

The connections in group “Dywidag” were reinforced by prestressing the timber laterally between the dowel and the loaded end (see 3.2.6). Figure 43 shows the load-slip behaviour for the three connections in group “Dywidag” where failure was reached, Figure 44 shows the measured lateral deformations. The average bearing capacity was  $F_{max} = 306$  kN with a coefficient of variation of  $CoV = 9,4$  %. The corresponding mean slip of the connection at  $F_{max}$  was  $\delta_{max} = 1,56$  mm. After failure an average residual strength of  $F_{res} = 90$  kN (29 %  $F_{max}$ ) was measured.

As the timber was prestressed laterally, no splitting prior to failure occurred in any of the connections. Figure 44 shows a linear behaviour for lateral deformations at the end. For specimen 13 a very small rate of lateral deformations was measured. Compared to the other five connections of the group the lateral stiffness  $k^{lat}$  for specimen 13 was more than a factor of 10 higher. Therefore, the measurements of lateral deformations in specimen 13 were considered not to be representative and were consequently not used to calculate mean values for lateral stiffness. Due to practical reasons, the lateral deformations near the dowel could not be measured.

The failure mode was combined shear plug and tensile failure (Figure 46). In specimens 13 and 14 the width of the shear plug was about twice the dowel diameter. In the areas between the dowel hole and the shear planes of the plug tensile failure occurred. In specimen 15 this kind of failure did not appear to the same extent, as the width of the shear plug was about equal to the dowel diameter and the area of tensile failure was significantly smaller than in specimens 13 and 14. Figure 43 shows a slightly ductile load-slip behaviour for all three connections, as the deformation rates increase before failure. Specimen 14 in particular showed larger deformations before the maximum load was reached.

Considering the data of all six connections involved in this test group – including the connections where failure was not reached - the following behaviour was observed for loads below bearing capacity:

No splitting was observed in any of the tested connections. The lateral deformations at the loaded end occurred at a mean lateral stiffness of  $k^{lat} = 100 \text{ kN/mm}$  (CoV = 8,3 %). Lateral deformations near the dowel were not measured. The lateral strain at the end reached an average value of  $\varepsilon = 0,83 \%$  (specimen 13 excluded). Considering the compression strains of  $\varepsilon = -3,5 \%$  due to prestressing, this means the timber remained in a compressed state during the complete test procedure.

For the load-slip behaviour of the dowel connection the stiffness was calculated to  $k^{split} = 311 \text{ kN/mm}$  (CoV = 5,4 %).

In Figure 45 the variation in the prestressing forces are shown for the three connections where failure occurred. The force in the Dywidag rods (P) correlates with the load applied to the dowel (F). The ratio  $\frac{\Delta P}{\Delta F} [\%]$  was calculated to display the increase of force in the Dywidag rods as a function of the load applied to the dowel. As can be seen in Figure 45 the ratio drops slightly for increasing loads F. However, the ratio is approximately constant for loads between  $F = 0,4F_{est} = 110 \text{ kN}$  and  $F = 0,7F_{est} = 190 \text{ kN}$ . In this range  $\frac{\Delta P}{\Delta F}$  was calculated for all six connections of the group and a mean value of  $\frac{\Delta P}{\Delta F} = 2,6 \%$  was obtained.

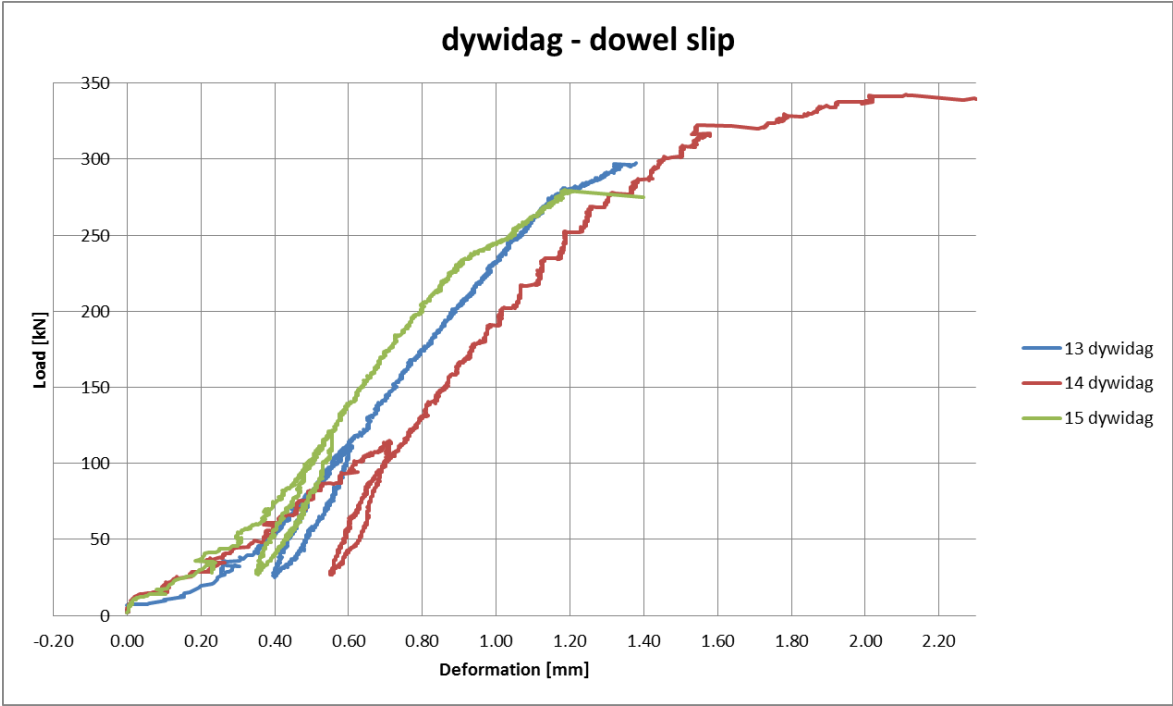


Figure 43 Load-slip behaviour in group "Dywidag".

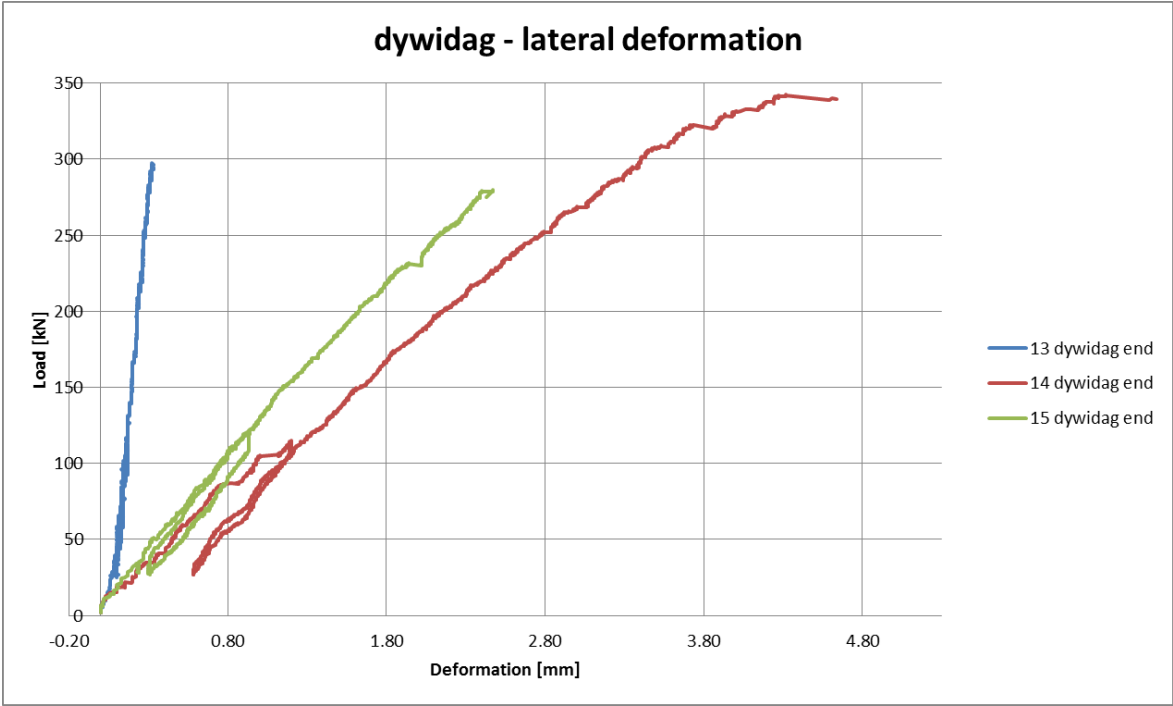


Figure 44 Load-lateral deformation behaviour in group "Dywidag".



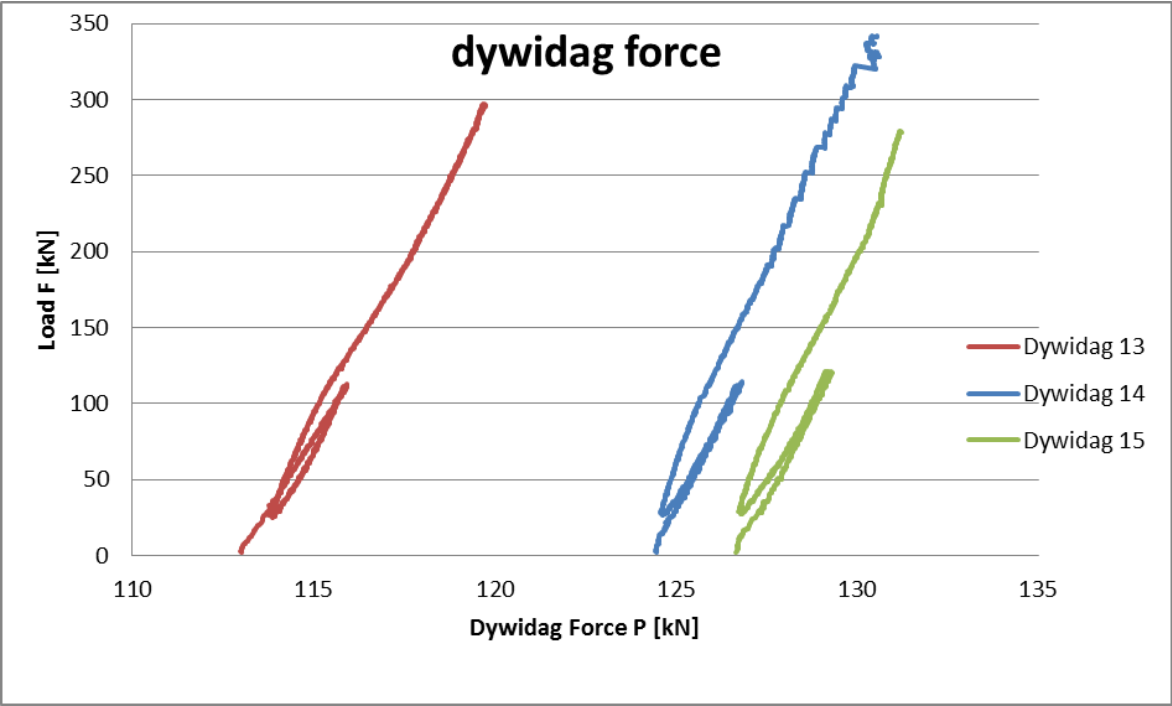


Figure 45 Prestressing forces in group "Dywidag".



Figure 46 Failure mode in specimen 13.

## 4.7 Summary of Test Results

Group	$F_{max}$ [kN]	CoV [%]	$\delta(F_{max})$ [mm]	$F_{res}/F_{max}$ [%]	$k^{slip}$ [kN/mm]	$\rho$ [kN/m <sup>3</sup> ]	MC [%]
"Basic"	134	4,1	0,48	~0	308	523	12,1
"A2+B2"	237	8,4	1,06	77	336	463	11,6
"02+A2"	187	8,9	1,24	60	360	473	10,9
"Inclined"	229	8,6	1,28	66	336	400	11,2
"Dywidag"	306	9,4	1,56	29	311	392	9,2

Table 6 Summary of test results.  $F_{max}$  is the bearing capacity of the connection, CoV the coefficient of variation for  $F_{max}$ ,  $\delta(F_{max})$  the dowel slip at  $F_{max}$ ,  $F_{res}/F_{max}$  is the ratio of residual strength to maximum load,  $k_{slip}$  the stiffness of the connection in load direction,  $\delta$  the density and MC the moisture content.

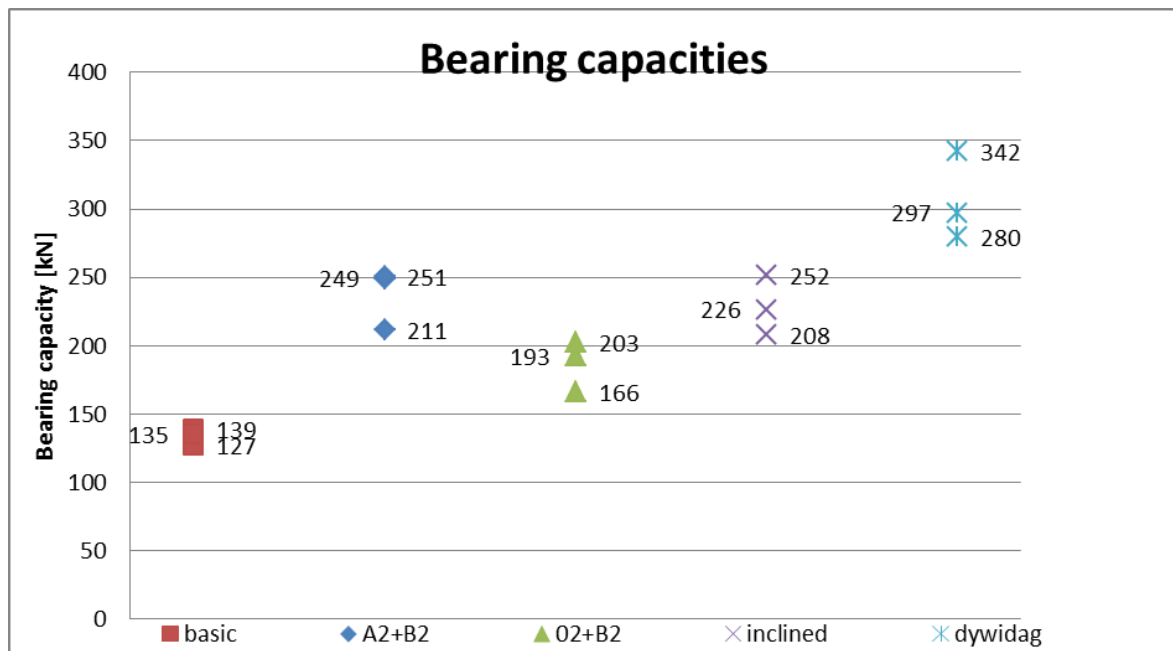


Figure 47 Bearing capacities [kN].

Table 6 displays average values of the test results for each group of specimens. As failure was only reached in one out of two connections per specimen the sample size for values associated with the bearing capacity ( $F_{max}$ ,  $\delta(F_{max})$ ,  $F_{res}$ ) is only three values per group. However, as explained in 4.1, the calculation of the coefficient of variation (CoV) was carried out with a sample size of six, assuming equal bearing capacities for both connections in each specimen. The average values for stiffness were calculated from six actual measurements per group.

### 4.7.1 Bearing Capacity

From Table 6 and Figure 47 it can be seen that the bearing capacity of the single dowel connections were significantly increased by the applied reinforcement measures. The gains in bearing capacity for the different specimen groups compared to non-reinforced connections (“Basic”) are:

- “A2+B2”: + 77 %
- “02+A2”: + 40 %
- “Inclined”: + 71 %
- “Dywidag”: + 128 %

The scatter in the results for bearing capacity (CoV) was between 8,4 ÷ 9,4 % in the reinforced groups and only 4,1 % in the non-reinforced group. However, these values have only a limited validity considering the small sample size of only three specimens per group.

The values of the residual strength  $F_{res}$  was about 60 ÷ 77 % of the maximum load for groups reinforced with self-tapping screws. For group “Dywidag” the value was only 29 % and the non-reinforced connections in group “Basic” showed almost no residual strength at all.

### 4.7.2 Failure Mode

The ultimate failure mode was a shear plug for all groups. The width of the plug was usually slightly smaller than the diameter of the dowel. An exception from this rule is group “Dywidag”, where the shear plug in two out of three connections was wider than the dowel diameter, implying also a change of the failure mode from shear failure to combined shear and tensile failure. This is discussed more in detail in 0.



Figure 48 Typical failure mode: shear plug.

### 4.7.3 Stiffness and Dowel Slip

As for the stiffness values  $k^{slip}$  a slight increase in stiffness of 9 ÷ 17 % was observed for the groups reinforced with screws (“A2+B2”, “02+A2” and “Inclined”) compared to the non-reinforced group. The prestressed connections in group “Dywidag” did not show any significant increase in stiffness.

However, the dowel slip at failure was the largest in group “Dywidag” ( $\delta(F_{max}) = 1,56$  mm), which was more than three times the slip in group “Basic” ( $\delta(F_{max}) = 0,48$  mm). Groups reinforced with screws also showed values of more than twice the slip in non-reinforced specimens at failure.

#### 4.7.4 Splitting and lateral stiffness

In Table 7 and Figure 49 the mean values of the load when splitting occurred ( $F_{\text{split}}$ ) and the corresponding lateral strains  $\varepsilon_{\text{split}}$  are listed. These mean values consist of the values from observed splitting prior to failure as well as the values at maximum load, since it is assumed that failure was initiated by splitting at maximum load. The groups which involve reinforcement screws placed towards the end (“A2+B2”, but also “Inclined”) showed higher values of  $F_{\text{split}}$  compared to group “Basic” without reinforcement, but also compared to group “02+A2” with reinforcements only near the dowel. In the prestressed specimens of group “Dywidag” no splitting was observed.

Group	$F_{\text{split}}$ [kN]	$\varepsilon_{\text{split}}$ [‰]	$k^{\text{lat}}$ [kN/mm]
"Basic"	105	2,76	93
"A2+B2"	199	4,05	115
"02+A2"	168	4,39	95
"Inclined"	204	4,12	121
"Dywidag"	-	-	100

Table 7 Mean values of splitting loads  $F_{\text{split}}$  and corresponding lateral strains  $\varepsilon_{\text{split}}$  as well as mean lateral stiffness values  $k^{\text{lat}}$ .

The lateral stiffness  $k^{\text{lat}}$  connects the load applied to the dowel with the lateral deformations measured at the loaded end of the connection. It can be seen that the groups with reinforcement screws towards the end (“A2+B2”, “Inclined”) showed significantly higher values for  $k^{\text{lat}}$  than groups without screws placed near the end (“Basic”, “02+A2”, “Dywidag”).

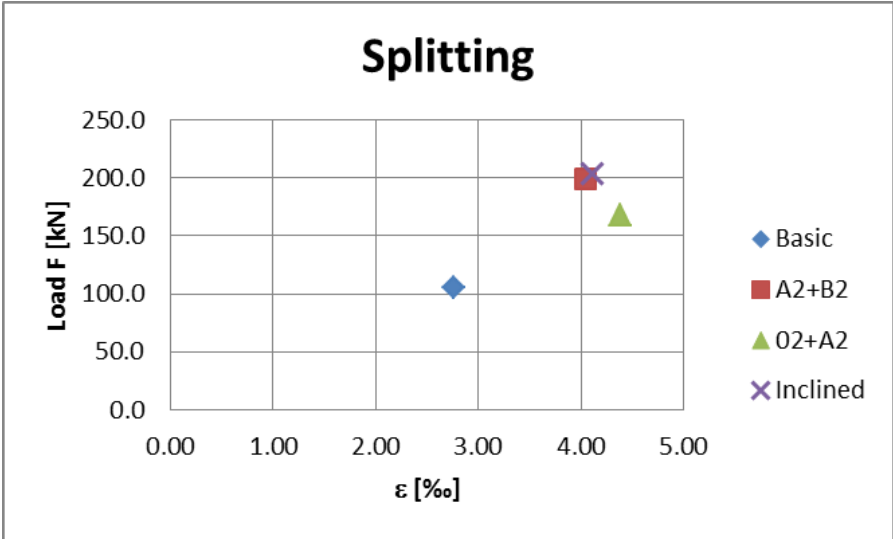


Figure 49 Mean values of  $F_{split}$  and  $\epsilon_{split}$  for the different groups. In group "Dywidag" no splitting occurred.



## 5 Discussion

### 5.1 Bearing Capacity and Lateral Deformations

#### 5.1.1 Connections Reinforced with Screws

A comparison of the groups using self-tapping screws shows that group “02+A2” achieved the least gain in bearing capacity. Groups “A2+B2” and “Inclined” showed a significantly larger improvement.

As shown in detail in 4.2 - 0, for all groups it was observed that substantial lateral deformations in the timber occurred at the loaded end, whereas close to the dowel deformations were only marginal. It was also observed that splitting had its origin at the loaded end of the connection. The lateral deformations in the connection are crucial to the attainable bearing capacity. Tensile stresses perpendicular to the grain lead to splitting and the formation of a shear plug is promoted. In group “02+A2” reinforcing screws were only placed near the dowel, thus there was no lateral reinforcement provided in the area towards the loaded end where the main expansion was measured. As a consequence, lateral expansion and splitting of the timber could not effectively be impeded using the configuration of group “02+A2” and the gain in bearing capacity was rather modest. As opposed to this, group “A2+B2” in particular - but also group “Inclined” - were equipped with screws positioned further away from the dowel. In that way, the timber was reinforced laterally in the area where lateral deformation actually did occur, allowing the reinforcement to counteract the expansion of the timber and the splitting tendency of the connection.

The finding that significant lateral expansion occurs at the end grain and almost no expansion or even compression is measured near the dowel can be comprehended by using a strut-and-tie model (Figure 50) to describe the stress distribution within the connection. The struts in the model entail the load parallel to the grain as well as the lateral load component transferred from the dowel. As seen from the figure, lateral tensile stresses at the end have to develop to provide equilibrium. Near the dowel, where the struts join, a narrow zone of compressive stress is formed. This distribution of lateral stresses does not conform to previous studies for



smaller dowels (Jorissen (1998), Bejtka (2005)) as presented in 2.1.2. So size effects seem to have an influence on lateral strains near the fastener. For smaller dowels ( $d \leq 20$  mm) a wedging effect of the dowel was observed which caused a split to form near the fastener (Jorissen, 1998). This was not observed in the large-dowel tests conducted in the course of this thesis.

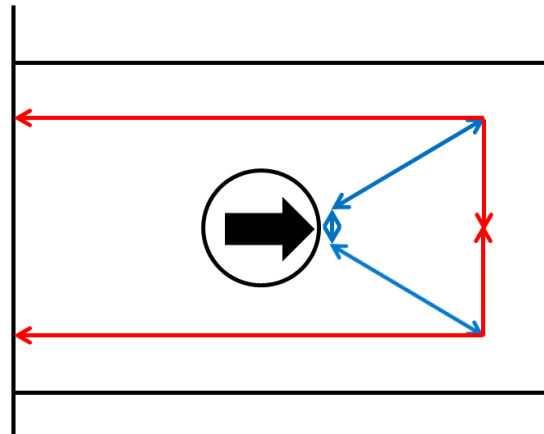


Figure 50 Qualitative strut-and-tie model. red: tensile stresses, blue: compression.

The influence of the reinforcements on lateral deformations can be illustrated by comparing the rate of lateral deformations at the loaded end as a function of the load applied to the dowel ( $k^{lat}$ ). Groups “Basic” and “02+A2” - where no lateral reinforcement in the area near the loaded end was applied - showed values of  $k^{lat} = 93$  kN/mm and  $k^{lat} = 95$  kN/mm respectively, whereas groups “A2+B2” and “Inclined” showed values of  $k^{lat} = 115$  kN/mm and  $k^{lat} = 121$  kN/mm. So the measured gain in lateral stiffness due to reinforcing screws lies between 22 % and 28 %.

Concerning the ultimate failure mode, the placement of the self-tapping screws did not seem to have any significant influence, since for all groups reinforced with screws the failure mode was a shear plug with a width equal to or somewhat smaller than the dowel diameter. Where splitting had occurred prior to failure it was observed that the initial split usually formed a shear plane of the plug. For specimens where no splitting prior to failure was observed it is assumed that the formation of the shear plug still was initiated by splitting (see 5.4). Excepted from this assumption are the specimens in group “Dywidag”, where splitting was excluded due to prestressing.

Given these results, it can be concluded that in order to increase the bearing capacity of single large-dowel connections with a reduced end distance, the self-tapping screws used as lateral reinforcements should be placed at the loaded end of the connection. However, although reinforcing screws effectively impede splitting, they cannot prevent the formation of a shear plug.

### 5.1.2 Prestressed Connections

The largest increase in bearing capacity however was achieved not by using self-tapping screws, but by lateral prestressing of the timber as in group “Dywidag”. Prestressing the timber at around 3,2 MPa ensured that no lateral tensile stresses occurred during the whole procedure of testing. This can be illustrated by the fact that during prestressing the timber was compressed to a strain of around 3,5 %, whereas the expansion during testing reached values of around 1 %. Splitting of the timber could thus be completely prevented. The lateral compression of the timber also increased the shear strength of the material along the grain. This means that the load parallel to the grain required to form a shear plug had to be higher in order to reach failure. It was observed that the prestressed connections showed a different failure mode than the connections reinforced with self-tapping screws. Whereas the non-prestressed connections developed a pure shear plug, the failure mode in the prestressed connections was a combined shear and tensile failure producing a wider plug. The change in the failure mode can be seen as a result of the increased shear strength along the grain due to prestressing, allowing to reach load levels where tensile failure in parts of the timber occurs before a shear plug is formed (see 5.4.3).

## 5.2 Stiffness

Table 6 also lists the stiffness values  $k^{slip}$  for the different groups. Groups reinforced with self-tapping screws (“A2+B2”, “02+A2”, “Inclined”) showed somewhat higher values of  $k^{slip}$  compared to groups without screws (“Basic”, “Dywidag”). For groups “A2+B2” and “02+A2” this can be explained referring to the screws placed in contact with the dowel, which act as an elastic foundation for the dowel, distributing the load to a wider area of the cross section and thus reducing stresses and strains parallel to the grain in the timber near the dowel. In group “Inclined” the screws are not in contact with the dowel. The increased

stiffness can be explained by the fact that the inclined screws add stiffness to the timber parallel to the grain, as the screws are subjected to axial forces when load parallel to the grain is applied. The reinforcements however had only a moderate influence on the stiffness values with gains of 9 % ÷ 17 %. In general it can be said that the deformations in load directions were rather small in all tests, with the maximum slip at failure  $\delta(F_{\max}) = 1,56$  mm reached in group “Dywidag”.

### 5.3 Comparison with Preliminary Test Series

The preliminary small-scale test series (Crocetti, Axelson, & Sartori, 2010) presented in 2.2 had shown that splitting was initiated at the end grain and that the ultimate failure mode was a shear plug, which was confirmed by the full-scale tests. However, in the small-scale tests the placing of the screws did not have an influence on the bearing capacity, whereas the full-scale tests showed that screws placed near the end were more effective than screws placed near the dowel. Furthermore, a more ductile failure was observed in the small-scale test as opposed to the rather brittle behaviour in the full-scale connections.

A reason for those differences can be found in the relative dimensions of the reinforcing screws compared to the timber member. The reinforcement screws used in the small-scale test had a diameter of  $d = 6,3$  mm. The cross section of the specimens was  $45$  mm  $\times$   $140$  mm. In the full-scale tests the screw diameter was  $d = 10$  mm and the cross section  $140$  mm  $\times$   $405$  mm. This gives the following relative dimensions:

- Ratio of the screw diameter  $d$  to the width  $t$  of the timber member:
  - Small-scale:  $\frac{t}{d} = \frac{45 \text{ mm}}{6,3 \text{ mm}} = 7,1$
  - Full-scale:  $\frac{t}{d} = \frac{140 \text{ mm}}{10 \text{ mm}} = 14,0$
- Slenderness of the screw (ratio of the height  $h$  of the timber member to the screw diameter):
  - Small-scale:  $\frac{h}{d} = \frac{140 \text{ mm}}{6,3 \text{ mm}} = 22,2$
  - Full-scale:  $\frac{h}{d} = \frac{405 \text{ mm}}{10 \text{ mm}} = 40,5$

Both ratios show about half the value in the small-scale tests. This means that the properties of the screws become more dominant in the compound material. A low ratio  $\frac{t}{d}$  leads to increased lateral stiffness and shear resistance. A small slenderness  $\frac{h}{d}$  of the screw means that its bending resistance has a bigger influence and adds more to the shear resistance at large deformation and thus leads to a more ductile failure.

## 5.4 Failure Process and Failure Mode

### 5.4.1 Simplified Model for Resistance Against Shear Failure

To analyse the results from the test series, a simple model is used to comprehend the process of failure and the differences in bearing capacities between different groups of reinforced specimens. As observed in the tests, the general ultimate failure mode is a shear plug with a width somewhat smaller than the dowel diameter. The model used in this chapter examines the influence of splitting on the bearing capacity by assuming constant shear stresses along the shear planes of the plug as well as a constant shear strength of the wood within the shear planes. The contribution of reinforcing screws to the shear resistance is neglected. For the following calculations, the shear strength of the timber is assumed to be  $f_v = 3,5 \text{ N/mm}^2$ .

Figure 51 shows the simplified model for pure shear failure with equal dimensions as in the tested specimens. Using this model, the resistance against the formation of a shear plug can be calculated by multiplying the area of both shear planes with the shear strength  $f_v$ .

The obtained resistance  $R$  of the connection for pure shear failure is

$$R_{\text{shear}} = 2 \times L \times t \times f_v = 2 \times 270\text{mm} \times 140\text{mm} \times 3,5 \text{ N/mm}^2 = 265 \text{ kN}.$$

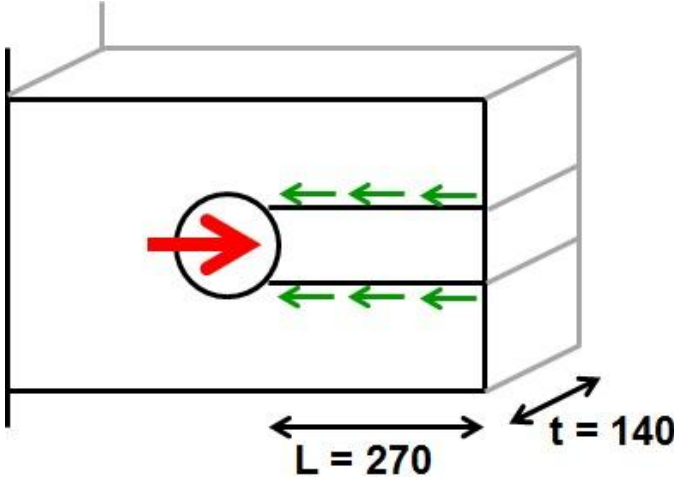


Figure 51 Simplified model for pure shear failure.

The value  $R_{\text{shear}}$  is the resistance of a connection where no splitting has occurred and therefore the shear strength of the wood contributes to the resistance on the whole area of both shear planes.

However, if splitting occurs prior to or at failure, the area contributing to the resistance is reduced and consequently the bearing capacity of the connection is lower than for pure shear failure ( $R_{\text{shear}}$ ):

$$R = [L + (L - L_{\text{split}})] \times t \times f_v,$$

$$R = [270\text{mm} + (270\text{mm} - L_{\text{split}})] \times 140\text{mm} \times 3,5 \text{ N/mm}^2 < R_{\text{shear}}.$$

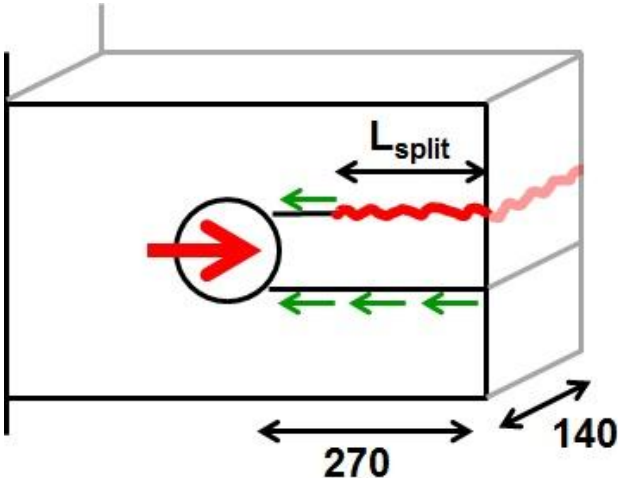


Figure 52 Simplified model with preliminary split.

**5.4.2 Comparison Between Groups “Basic” and “A2+B2”**

In order to study the influence of the splitting behaviour on the bearing capacity of a connection, the simplified model introduced in 5.4.1 is used to compare group “Basic” with group “A2+B2”. As was observed during testing, splitting is initiated at the loaded end of the connections. Group “Basic” is the non-reinforced group, whereas group “A2+B2” is reinforced by screws inserted perpendicular to the grain. In particular the specimens in group “A2+B2” are reinforced with screws near the loaded end, where significant lateral deformations occur and splitting is initiated.

These two groups were chosen for comparison to study the influence of reinforcing screws placed near the end as opposed to connections without reinforcement.

The average bearing capacity for group “Basic” in the tests was  $F_{max} = 134 \text{ kN}$ . As splitting was observed prior to failure, the resistance of the connection is reduced compared to pure shear failure  $R_{shear} = 265 \text{ kN}$ . Assuming the split ranging all the way from the end to the dowel, the resistance of the connection drops to half of the value of  $R_{shear}$  (Figure 53). The resistance in group “Basic” can thus be calculated to

$$R = L \times t \times f_v = 270 \text{ mm} \times 140 \text{ mm} \times 3,5 \text{ N/mm}^2 = 132 \text{ kN} \approx F_{max} = 134 \text{ kN}.$$

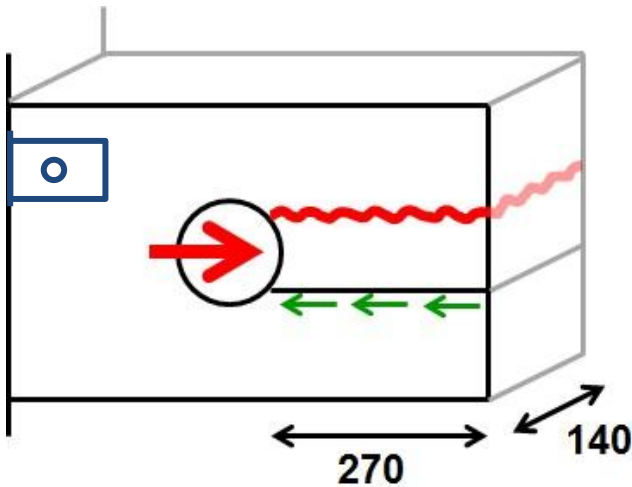


Figure 53 Simplified model for group "Basic".

In group “A2+B2” the measured average bearing capacity was  $F_{\max} = 237$  kN. Although splitting was impeded by the reinforcing screws it could not be completely prevented. Back-calculation from the measured value of  $F_{\max}$  gives the theoretical crack length at failure:

$$R = F_{\max} = [L + (L - L_{\text{split}})] \times t \times f_v$$

$$\rightarrow L_{\text{split}} = 2 \times L - \frac{F_{\max}}{t \times f_v} \approx 55 \text{ mm.}$$

This means that the crack length is reduced by the applied reinforcing screws.

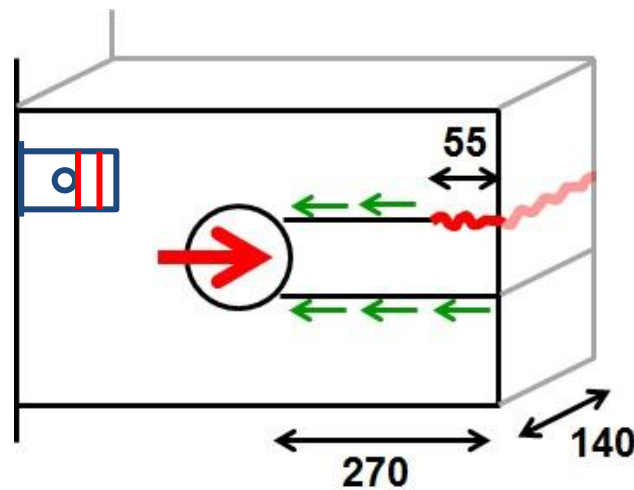


Figure 54 Simplified model for group "A2+B2".

To better understand the difference in the failure process between reinforced and non-reinforced connections the differing splitting behaviour of the groups has to be considered. The single dots in Figure 55 stand for the measured values at splitting in both groups. The average values within the groups are marked with an “X” and lead to the average splitting loads  $F_{\text{split}}$  [kN] as well as to the corresponding lateral strains  $\varepsilon_{\text{split}}$  [‰]. Furthermore, the lateral stiffnesses are shown qualitatively as the gradient of the linearised load-strain curves.

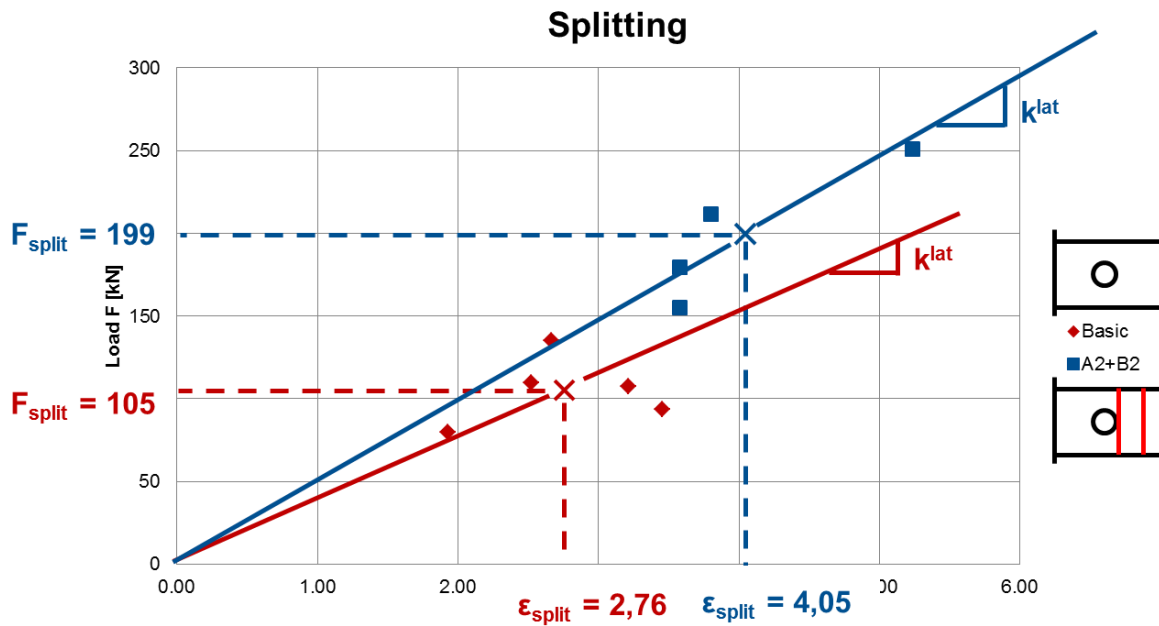


Figure 55 Splitting behaviour of groups "Basic" and "A2+B2".

As shown in Figure 55, splitting in the reinforced group "A2+B2" occurs at a higher load  $F_{\text{split}}$  but also at a higher lateral strain  $\epsilon_{\text{split}}$ . Parts of the increase in the splitting load  $F_{\text{split}}$  can be explained by the larger lateral stiffness  $k^{\text{lat}}$  of the reinforced group. This means that the lateral strains  $\epsilon$  are smaller in group "A2+B2" than in group "Basic" for an equal load  $F$ . As splitting depends on the lateral strains this consequently leads to a higher splitting load  $F_{\text{split}}$ .

However, it can also be observed that splitting occurs at higher lateral strains in the reinforced connections, which cannot be explained by the differences in the overall lateral stiffness  $k^{\text{lat}}$ . The measured values of  $\epsilon$  are the mean lateral strains over the height of the specimen derived from measuring the total deformation from edge to edge. They do not give any information about the distribution of the strains within the material. As timber is a natural material its properties show a significant variation within the same specimen. The lateral strains are not constant over the height of the specimen but will predominantly occur in weaker parts of the wood, i.e. in areas of lower lateral stiffness. Thus, the maximum local strains are higher than the measured average strains and splitting is bound to occur in these areas of large local strains.

Adding reinforcing screws does not have an influence on the properties of the timber but certainly on the compound material of timber and screws. As opposed to wood, the



manufactured screws have more or less constant properties of strength and stiffness. Thus, inserting screws into the wood does not only enhance strength and stiffness values, it also evens out the natural scatter of material properties. Consequently, the variation of lateral strains within the material is reduced and local strain peaks are flattened. This allows a larger total lateral deformation and therefore also larger average lateral strains before splitting occurs. This in turn leads to a higher splitting load  $F_{split}$ . Furthermore, the screws provide a lateral strength in the material even after splitting, restricting the crack propagation from the end towards the dowel.

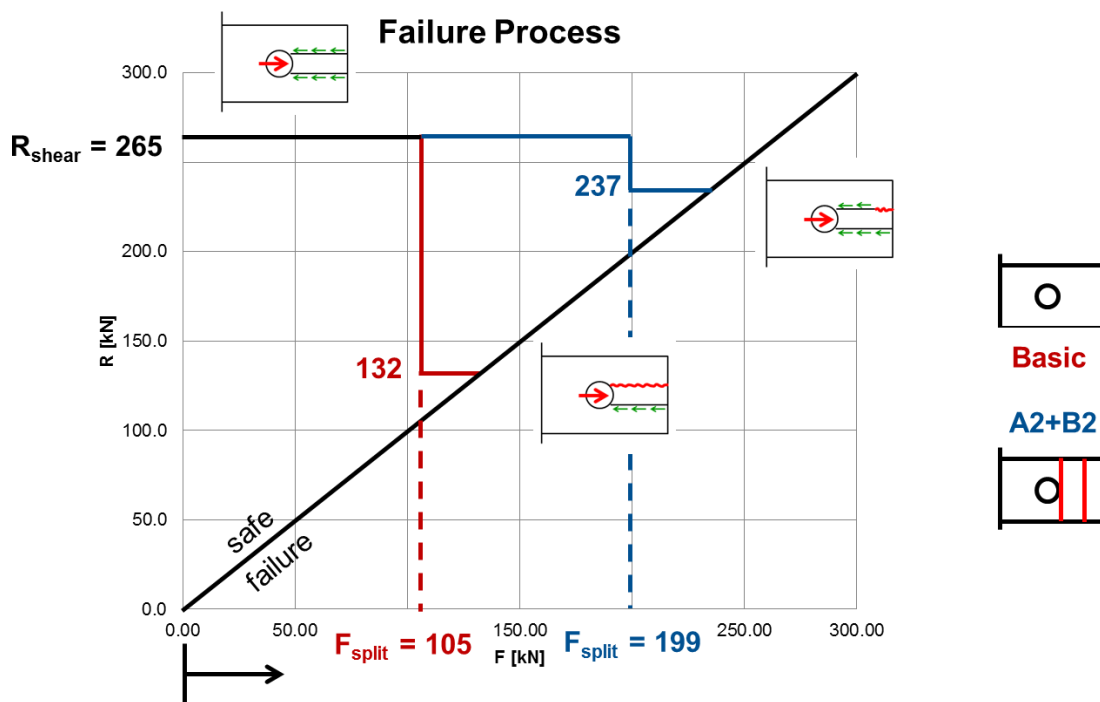


Figure 56 Process of failure for groups "Basic" and "A2+B2".

Figure 56 visualises the process of failure for the groups examined with the simplified model. When starting to increase the load  $F$  on the abscissa, both connections show the full value of shear resistance  $R_{shear}$  until the critical splitting load for group "Basic" is reached. The resistance of the non-reinforced connection then drops to half of the original value, allowing only a moderate increase in load before failure occurs. In the reinforced group "A2+B2" splitting occurs at a significantly higher load level and the loss in resistance is much smaller due to the limited crack length.

Figure 56 shows the failure process using mean values of the groups, which leads to the result that splitting occurs at a critical splitting load  $F_{split}$  which is smaller than the maximum load  $F_{max} = R$  where failure occurs. However, if for example the individual results in the reinforced group “A2+B2” are considered, it can be seen that only in one out of three failed connections splitting occurred prior to failure ( $F_{split} < F_{max}$ ). In the two other connections failure occurred without visible or detected preliminary splitting. In consistency with the resistance model introduced above it can still be assumed that the formation of the shear plug is initiated by splitting, only that the splitting load  $F_{split}$  is now equal to the bearing capacity  $F_{max}$ . The change from a failure process with  $F_{split} < F_{max}$  to a process with  $F_{split} = F_{max}$  is dependent on two factors: the split length, which determines the loss in resistance, and the load level at splitting. These influences are visualised qualitatively in Figure 57. The solid line denotes the failure process with preliminary splitting ( $F_{split} < F_{max}$ ) as derived from the mean values and the dotted lines show two modifications of the failure process without preliminary splitting ( $F_{split} = F_{max}$ ) depending on the two factors mentioned above. Modification 1 shows the failure process for an increased split length leading to a greater loss in resistance. For a large enough split the resistance of the connection drops below the load level  $F$  and the shear plug is formed immediately after splitting. Modification 2 shows the influence of an increased splitting force  $F_{split}$ . The closer the applied load  $F$  gets to the maximum shear resistance  $R_{shear}$  of the connection, the smaller the loss in resistance due to splitting has to be in order to lead to failure immediately. So if a split appears at a low load level  $F$  the connection might still stay intact, while an equal split occurring at a higher load will lead to immediate failure.

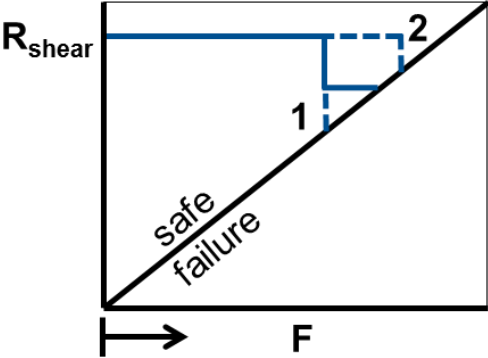


Figure 57 Variations in the failure process.

### 5.4.3 Failure Modes in Prestressed Connections

In the prestressed connections of group “Dywidag” no splitting was observed. As described in 3.2.6 the specimens were compressed to strains of about  $\varepsilon = - 3,5 \%$  during prestressing. The lateral expansion during testing reached only values of  $\varepsilon = + 0,83 \%$ , so it can safely be stated that no lateral tensile stresses occurred during testing and splitting could be completely prevented.

Using the model presented in 5.4.1, this means the full resistance  $R_{\text{shear}}$  for pure shear failure is mobilised (Figure 51). By again assuming a shear strength of  $f_v = 3,5 \text{ N/mm}^2$  the resistance for a split-free connection with a shear plug slightly smaller than the dowel diameter is calculated to  $R_{\text{shear}} = 265 \text{ kN}$ . This predicted failure mode was observed in specimen no. 15 of group “Dywidag” (Figure 58). The measured maximum load was  $F_{\text{max},15} = 280 \text{ kN}$ , which is slightly higher than predicted resistance of  $R_{\text{shear}} = 265 \text{ kN}$  by the model but certainly is in the same magnitude.



Figure 58 Shear plug in prestressed specimen no. 15.

However, for the other two specimens (no. 13 and 14) in the group significantly higher bearing capacities of  $F_{\text{max},13} = 297 \text{ kN}$  and  $F_{\text{max},14} = 342 \text{ kN}$  respectively were measured. Moreover, a change in the failure mode was observed. Instead of a pure shear failure a combined shear and tensile failure occurred (Figure 59).



Figure 59 Combined shear and tensile failure in prestressed specimen no. 14.

In the following paragraphs an idea to explain the change in the failure mode is presented:

The idea is based on the assumption that the shear strength  $f_v$  is increased by prestressing (Figure 60). As the tensile strength  $f_t$  is assumed to be independent from lateral stresses, an increased shear strength lowers the ratio  $\frac{f_t}{f_v}$  between the tensile strength and the shear strength, which eventually allows new failure modes to form.

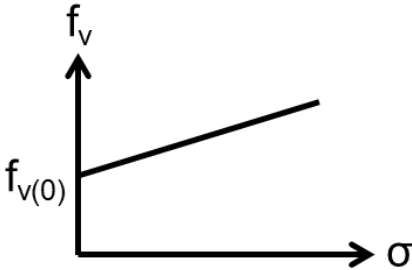


Figure 60 Assumed increase in shear strength  $f_v$  due to prestress  $\sigma$ .

The idea shall be illustrated by a simplified qualitative model. The presented calculations are not meant to represent actual results observed in the tests. They are rather used to help illustrating the presented idea.

It is assumed that the shear strength within the wood shows a natural scatter. The influence of the average shear strength level on the failure mode is analysed for one specific hypothetical distribution of shear strength.

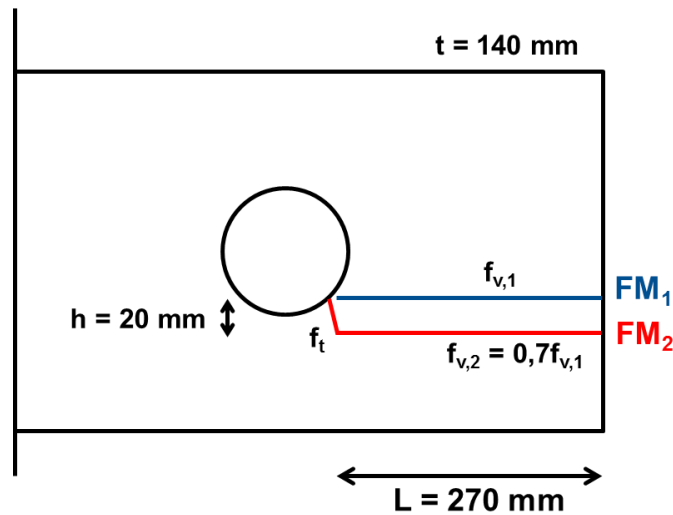


Figure 61 Assumed situation for failure mode analysis.

Figure 61 shows the assumed situation. Two different failure modes are considered. Failure mode  $FM_1$  represents the pure shear failure.  $FM_2$  represents a combined shear and tensile failure.

First, the failure modes are studied for a normal shear strength level: As yet, the shear strength is set to  $f_{v,1} = 3,5 \text{ N/mm}^2$ . It is assumed that due to the natural scatter the shear strength at a distance of  $h = 20 \text{ mm}$  from  $FM_1$  is only 70 % of  $f_{v,1}$ , i.e.  $f_{v,2} = 0,7 \times f_{v,1} = 2,5 \text{ N/mm}^2$ . The tensile strength is set to  $f_t = 20 \text{ N/mm}^2$ . Given these assumption the resistance of both possible failure modes can be calculated to

$$R_1 = L \times t \times f_{v,1} = 270 \text{ mm} \times 140 \text{ mm} \times 3,5 \text{ N/mm}^2 = 132 \text{ kN} \text{ and}$$

$$R_2 = L \times t \times f_{v,2} + h \times t \times f_t,$$

$$R_2 = 270 \text{ mm} \times 140 \text{ mm} \times 2,5 \text{ N/mm}^2 + 20 \text{ mm} \times 140 \text{ mm} \times 20 \text{ N/mm}^2 = 151 \text{ kN}.$$

$$\rightarrow R_1 < R_2$$

The resistance  $R_1$  being smaller than  $R_2$  means that failure mode  $FM_1$  (pure shear failure) is bound to occur, even though its shear strength is higher than in the potential shear plane of  $FM_2$ .

Next, the same failure modes are examined for an enhanced shear stress level: The shear strength for FM<sub>1</sub> is now assumed to be increased due to prestressing to a value of  $f_{v,1} = 5,0$  N/mm<sup>2</sup>. Again  $f_{v,2}$  is set to 70 % of  $f_{v,1}$ , i.e.  $f_{v,2} = 3,5$  N/mm<sup>2</sup>. The tensile strength is not influenced by prestressing and remains therefore at a value of  $f_t = 20$  N/mm<sup>2</sup>. Again the resistance is calculated for both failure modes:

$$R_1 = L \times t \times f_{v,1} = 270 \text{ mm} \times 140 \text{ mm} \times 5,0 \text{ N/mm}^2 = 189 \text{ kN and}$$

$$R_2 = L \times t \times f_{v,2} + h \times t \times f_t$$

$$R_2 = 270 \text{ mm} \times 140 \text{ mm} \times 3,5 \text{ N/mm}^2 + 20 \text{ mm} \times 140 \text{ mm} \times 20 \text{ N/mm}^2 = 188 \text{ kN.}$$

$$\rightarrow R_1 > R_2$$

This time the resistance of FM<sub>2</sub> is marginally smaller, which means that the failure mode has now changed from a pure shear failure to a combined shear and tensile failure.

By enhancing the overall shear strength level the resistance is increased for both possible failure modes. However, since the ratio  $\frac{f_t}{f_v}$  between the tensile strength and the shear strength is reduced, the contribution of the area of tensile failure is becoming less significant. This engenders, that for an increased overall shear stress level (i.e. a lower ratio  $\frac{f_t}{f_v}$ ) the combined shear and tensile failure becomes possible, whereas the failure mode for a lower shear stress level will always be pure shear failure.

From this qualitative analysis it can be concluded that if prestressing enhances the overall shear strength level, then a higher level of prestressing would even further enhance the bearing capacity. This would mean that the purpose of prestressing goes beyond preventing the timber to split and that it also adds resistance to the connection by enhancing the shear strength of the wood. Further it can be stated that prestressing a connection can change the failure mode from shear failure to a combined shear and tensile failure.

Theoretically, it should be possible to increase the bearing capacity of the connection by a higher level of prestress until a failure mode of pure tensile failure is reached. However, applying even higher levels of prestress than in the conducted test series would involve extensive crunching of the wood fibres and thus large deformations due to prestressing as well as increased relaxation after the application of the prestressing force, which would question the feasibility in practice.

## 6 Conclusions and Future Work

From the results of the full-scale test series for single large-dowel connections the following conclusions can be drawn:

- Major lateral strains occur at the loaded end of the connection and thus splitting is initiated at the end grain.
- Self-tapping reinforcement screws inserted perpendicularly to the grain impede splitting and can thus significantly enhance the bearing capacity.
- Reinforcing screws are most effective if placed near the end grain, where the main lateral deformations occur.
- Reinforcing screws cannot prevent the formation of a shear plug, which is the ultimate failure mode.
- Lateral prestressing is suitable for preventing splitting and enhancing the bearing capacity of a connection.

From the observation that splitting is initiated at the end grain, further studies should focus on reinforcements near the loaded end of the connection.

In order to better understand the influence of prestressing on the behaviour of the connection, further test with different levels of prestress could be carried out.

For further analysis of the stress distribution within the connection, strut-and-tie models as in Figure 50 (5.1.1) could prove to be a useful tool, especially for determining lateral stresses and to define required reinforcements.

By using the information from the test series, a finite element model could be developed to predict failure and stiffness of the connection.





## 7 References

- Awaludin, A., Hirai, T., Hayashikawa, T., & Sasaki, Y. (2008). Load-carrying capacity of steel-to-timber joints with a pretensioned bolt. *J Wood Sci (2008) 54*, pp. 362-368.
- Bejtka, I. (2005). *Verstärkung von Bauteilen aus Holz mit Vollgewindeschrauben*. Universitätsverlag Karlsruhe.
- Bejtka, I., & Blass, H. J. (2005). *Self-tapping screws as reinforcements in connections with dowel-type fasteners*. CIB W18 - Timber Structures. Meeting 18, Karlsruhe, Germany.
- Blass, H. J. (2003). Joints with Dowel-type Fasteners. In S. Thelandersson, & H. J. Larsen, *Timber Engineering* (pp. 315-331). John Wiley & Sons Ltd.
- Blass, H. J., & Bejtka, I. (2008). *Numerische Berechnung der Tragfähigkeit und der Steifigkeit von querzugverstärkten Verbindungen mit stiftförmigen Verbindungsmitteln*. Universitätsverlag Karlsruhe.
- Blass, H. J., & Schmid, M. (2001). *Self-tapping Screws as Reinforcement Perpendicular to the Grain in Timber Connections*. University of Karlsruhe.
- BST Byggstandardiseringen. (1991). *EN 26 891:1991, Timber structures - Joints made with mechanical fasteners - General Principles for the determination of strength and deformation characteristics*. SIS.
- Crocetti, R., Axelson, M., & Sartori, T. (2010). *Strengthening of large diameter single woel joints*. Borås: SP Technical Research Institute of Sweden.
- Dahl, K. B. (2009). *Mechanical properties of clear wood from Norway spruce*. Trondheim: Norwegian University of Science and Technology.

- Daudeville, L., Davenne, L., & Yasumura, M. (1999). Predictions of the load carrying capacity of bolted timber joints. *Wood Science and Technology* 33, pp. 15-29.
- Johansen, K. W. (1949). Theory of timber connections. *Int. Assn. of Bridge and Struct. Engrg. J.*, 9, pp. 249-262.
- Jorissen, A. (1998). *Double Shear Timber Connections with Dowel Type Fasteners*. Delft University Press.
- Martin, B. T., & Sanders, D. H. (2007). *Verification and Implementation of Strut-and-Tie Model in LRFD Bridge Design Specifications*. American Association of State Highway and Transportation Officials (AASHTO).
- Pedersen, M. U. (2002). *Dowel Type Timber Connections - Strength Modelling*. Danmarks Tekniske Universitet.
- Soltis, L. A., Karnasudirdja, S., & Little, J. K. (1987, January). Angle to Grain Strength of Dowel-Type Fasteners. *Wood and Fibre Science*, 19(1), 1987, pp. 68-80.
- Zhou, T., & Guan, Z. (2006). Review of existing and newly developed approaches to obtain timber embedding strength. *Prog. Struct. Engng Mater*, 8, 2006, pp. 46-67.

## **8 Appendix**

### **A1 Bearing Capacities**

### **A2 Stiffness Values (Load – Dowel Slip)**

### **A3 Splitting**

### **A4 Lateral Stiffness**

### **A5 Densities and Moisture Contents**

### **A6 Failure Modes**

## A1 Bearing Capacities

Specimen group and no.	Bearing capacity $F_{max}$			Dowel slip at $F_{max}$		Lateral deformation at $F_{max}$						Residual strength $F_{res}$				
	$F_{max}$ [kN]	$F_{max,mean}$ [kN]	COV [%]	$\delta(F_{max})$ [mm]	$\delta(F_{max})^{mean}$ [mm]	End			Dowel			$F_{res}$ [kN]	$F_{res,mean}$ [kN]	$\left(\frac{F_{res}}{F_{max}}\right)^{mean}$ [%]		
						$\delta_{lat}^{end}$ [mm]	$\delta_{lat,mean}^{end}$ [mm]	$\varepsilon_{lat,mean}^{end}$ [‰]	$\delta_{lat}^{dowel}$ [mm]	$\delta_{lat,mean}^{dowel}$ [mm]	$\varepsilon_{lat,mean}^{dowel}$ [‰]					
"Basic"	1	139		0.46		2.15			0.00			~0				
	2	127	4.1	0.73	0.48	3.08	2.10	5.19	0.59	0.25	0.63	~0	~0	~0		
	3	135		0.26		1.08			0.17			~0				
"A2+B2"	4	211		0.89		1.54			-0.04			207				
	5	249	8.4	0.97	1.06	3.94	2.53	6.26	-0.01	0.22	0.55	166	183	77		
	6	251		1.33		2.12			0.72			177				
"02+A2"	7	193		0.63		1.90			0.21			124				
	8	203	8.9	1.11	1.24	-	3.32	8.20	-	1.98	4.88	84	112	60		
	9	166		2.00		8.06			5.72			127				
"Inclined"	10	208		1.28		4.73			1.14			155				
	11	252	8.6	1.00	1.28	1.77	2.84	7.00	-0.13	0.62	1.54	139	151	66		
	12	226		1.58		2.01			0.86			160				
"Dywidag"	13	297		1.38		0.32			-			40				
	14	342	9.4	2.11	1.56	4.27	2.35	5.81	-	-	-	103	90	29		
	15	280		1.19		2.47			-			126				

**A2 Stiffness Values (Load – Dowel Slip)**

Specimen group and no.		Stiffness (load - dowel slip)		
		k [kN/mm]	k <sub>mean</sub> [kN/mm]	CoV [%]
"Basic"	1	<b>318</b> 279	308	15.2
	2	<b>260</b> 371		
	3	<b>354</b> 269		
"A2+B2"	4	<b>313</b> 387	336	8.7
	5	<b>348</b> 308		
	6	<b>339</b> 322		
"02+A2"	7	<b>374</b> 361	360	11.4
	8	<b>389</b> 318		
	9	<b>413</b> 307		
"Inclined"	10	<b>279</b> 350	336	15.2
	11	<b>324</b> 414		
	12	<b>285</b> 363		
"Dywidag"	13	<b>302</b> 333	311	5.4
	14	<b>299</b> 310		
	15	<b>331</b> 293		

Annotations: Values for k printed in bold are values from the failed connections, normally printed values are from the connection in the specimen which stayed intact.

**A3 Splitting**

Specimen group and no.		Splitting load $F_{split}$		Lateral deformation at end at $F_{split}$		
		$F_{split}$ [kN]	$F_{split,mean}$ [kN]	$\delta_{split,end}$ [mm]	$\epsilon_{split}$ [‰]	$\epsilon_{split,mean}$ [‰]
"Basic"	1	110 94	105	1.02 1.40	2.52 3.46	2.76
	2	80 -		0.78 -	1.93 -	
	3	<b>135</b> 108		<b>1.08</b> 1.30	<b>2.67</b> 3.21	
"A2+B2"	4	<b>211</b> -	199	<b>1.54</b> -	<b>3.80</b> -	4.05
	5	180 155		1.45 1.45	3.58 3.58	
	6	<b>251</b> -		<b>2.12</b> -	<b>5.23</b> -	
"02+A2"	7	<b>193</b> 173	168	<b>1.90</b> 2.15	<b>4.69</b> 5.31	4.39
	8	163 -		1.43 -	3.53 -	
	9	142 -		1.63 -	4.02 -	
"Inclined"	10	133 -	204	1.22 -	3.01 -	4.12
	11	<b>252</b> -		<b>1.77</b> -	<b>4.37</b> -	
	12	<b>226</b> -		<b>2.01</b> -	<b>4.96</b> -	
"Dywidag"	13	- -	-	- -	- -	-
	14	- -		- -	- -	
	15	- -		- -	- -	

Annotations: Values printed in bold signify splitting at failure ( $F_{split} = F_{max}$ )

**A4 Lateral Stiffness**

Specimen group and no.		Lateral stiffness at end		
		$k^{lat}$	$k_{mean}^{lat}$	CoV
		[kN/mm]	[kN/mm]	[%]
"Basic"	1	96 85	93	21.2
	2	67 115		
	3	116 79		
"A2+B2"	4	130 130	115	10.8
	5	110 105		
	6	115 100		
"02+A2"	7	94 74	95	21.3
	8	107 75		
	9	94 128		
"Inclined"	10	106 111	121	17.2
	11	142 153		
	12	106 108		
"Dywidag"	13	(1171)* 101	100	8.3
	14	87 98		
	15	103 110		

\*Considered as measurement error, not used for calculating mean values.



## A5 Densities and Moisture Contents

Specimen group and no.		Densities [kg/m <sup>3</sup> ]				Moisture content [%]	
		$\rho_{ave}$	$\rho_{ave,mean}$	$\rho_{fail}$	$\rho_{fail,mean}$	MC	MC <sub>mean</sub>
"Basic"	1	480	483	566	523	12.4	12.1
	2	482		474			
	3	486		528			
"A2+B2"	4	465	463	471	463	12.1	11.6
	5	481		548			
	6	444		370			
"02+A2"	7	452	451	471	473	11.0	10.9
	8	460		485			
	9	443		465			
"Inclined"	10	458	457	385	400	11.0	11.2
	11	455		460			
	12	458		356			
"Dywidag"	13	464	450	380	392	8.9	9.2
	14	450		403			
	15	437		395			

Annotations:

$\rho_{ave}$ : Average density of a whole specimen derived from its weight and dimensions.

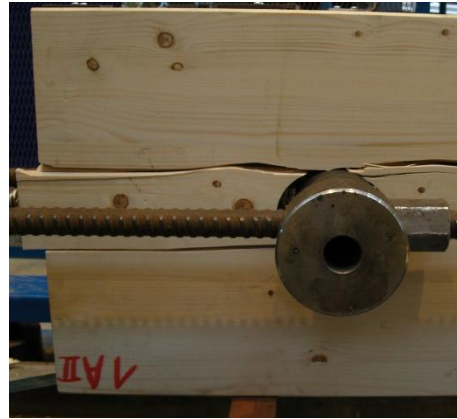
$\rho_{fail}$ : Densities from density tests of one single sample per specimen, taken from the part of the specimen where failure had occurred, i.e. from the shear plug.

MC: Moisture contents obtained from tests of one single sample per specimen, taken from the shear plug (same sample as used for  $\rho_{fail}$ ).

**A6 Failure Modes**

**Group “Basic”**

Specimen no. 1



Specimen no. 2



Specimen no. 3



**Group “A2+B2”**

Specimen no. 4



Specimen no. 5



Specimen no. 6



**Group “02+A2”**

Specimen no. 7



Specimen no. 8



Specimen no. 9



### Group “Inclined”

Specimen no. 10



Specimen no. 11



Specimen no. 12



**Group “Dywidag”**

Specimen no. 13



Specimen no. 14



Specimen no. 15

